



OPEN ACCESS

EDITED BY

Bin Xia,
Qingdao Agricultural University, China

REVIEWED BY

Maocang Yan,
Zhejiang Mariculture Research Institute, China
Ting Chen,
Chinese Academy of Sciences (CAS), China

*CORRESPONDENCE

Chuanyan Yang
✉ yangchuanyan@drou.edu.cn
Lingling Wang
✉ wanglingling@drou.edu.cn

RECEIVED 19 February 2024

ACCEPTED 28 March 2024

PUBLISHED 24 May 2024

CITATION

Ma X, Gu W, Yang C, He Z, Fan H, Wang L and Song L (2024) Inhibition of TRPA1-like alleviated unfolded protein response and apoptosis by regulating cytoplasmic Ca²⁺ in Yesso scallop *Patinopecten yessoensis* under high temperature stress.
Front. Mar. Sci. 11:1388382.
doi: 10.3389/fmars.2024.1388382

COPYRIGHT

© 2024 Ma, Gu, Yang, He, Fan, Wang and Song. This is an open-access article distributed under the terms of the [Creative Commons Attribution License \(CC BY\)](https://creativecommons.org/licenses/by/4.0/). The use, distribution or reproduction in other forums is permitted, provided the original author(s) and the copyright owner(s) are credited and that the original publication in this journal is cited, in accordance with accepted academic practice. No use, distribution or reproduction is permitted which does not comply with these terms.

Inhibition of TRPA1-like alleviated unfolded protein response and apoptosis by regulating cytoplasmic Ca²⁺ in Yesso scallop *Patinopecten yessoensis* under high temperature stress

Xiaoxue Ma^{1,2}, Wenfei Gu^{1,2}, Chuanyan Yang^{1,2*}, Zhaoyu He^{1,2}, Hongmei Fan^{1,2}, Lingling Wang^{1,2,3*} and Linsheng Song^{1,2,3,4}

¹Liaoning Key Laboratory of Marine Animal Immunology & Disease Control, Dalian Ocean University, Dalian, China, ²Dalian Key Laboratory of Aquatic Animal Disease Prevention and Control, Dalian Ocean University, Dalian, China, ³Laboratory of Marine Fisheries Science and Food Production Processes, Qingdao National Laboratory for Marine Science and Technology, Qingdao, China, ⁴Southern Marine Science and Engineering Guangdong Laboratory (Zhuhai), Zhuhai, China

Transient receptor potential ankyrin subtype 1 (TRPA1) is a nonselective cation channel protein typically forms ion channels that regulate intracellular calcium homeostasis, and can be induced by temperature and various chemicals. In the present study, the involvement of PyTRPA1-like in regulating unfolded protein response (UPR) and apoptosis in Yesso Scallop *Patinopecten yessoensis* under high temperature stress was investigated. The mRNA transcripts of PyTRPA1-like were detected in haemocytes and all the examined tissues with the highest expression level in mantle. After TRPA1 activator (allyl-isothiocyanate, AITC) and high temperature (25°C) treatment, the expression level of PyTRPA1-like mRNA and the Ca²⁺ content in haemocytes increased significantly ($p < 0.05$) at 3 h, and then recovered to the normal level at 12 h, and the expression level of PyGRP78, PyIRE1, PyATF6 β , PyPERK and PyCaspase-3 mRNA in haemocytes, and Caspase-3 activity and apoptosis rate were also significantly upregulated ($p < 0.05$). After TRPA1 antagonist (HC-030031) and high temperature (25°C) treatment, the intracellular Ca²⁺ content, the transcripts of PyGRP78, PyIRE1 and PyCaspase-3 in haemocytes, as well as the Caspase-3 activity and apoptosis rate decreased significantly compared to the control group ($p < 0.05$), while the Ca²⁺ distribution in haemocytes showed no difference with that in control group. These results collectively suggest that PyTRPA1-like plays important roles in regulating UPR and apoptosis by mediating calcium influx under high temperature stress in scallop *P. yessoensis*.

KEYWORDS

Patinopecten yessoensis, transient receptor potential ankyrin 1 channel, calcium ion, high temperature, unfolded protein response, apoptosis

1 Introduction

Transient receptor potential (TRP) channel, a class of non-selective cation channel proteins, typically form ion channels that regulate intracellular calcium homeostasis (Logashina et al., 2019). According to their structural characteristics, the TRP superfamily is divided into seven subfamilies, including TRPA (Ankyrin-like with transmembrane domains), TRPC (Canonical or Classical), TRPM (Melastatin), TRPML (Mucolipin), TRPN (No mechanoreceptor potential C), TRPP (Polycystin), and TRPV (Vanilloid receptor) (Logashina et al., 2019). Among them, TRPA1, first isolated from human lung fibroblasts in 1999 (Jaquemar et al., 1999), is a nonselective cation channel that allows passage of monovalent and divalent ions such as Ca^{2+} , Na^+ , and K^+ (Naert et al., 2020), exhibiting a higher permeability to Ca^{2+} compared to other TRP channels (Nilius and Owsianik, 2011; Nilius et al., 2012).

TRPA1 channels are prevalent and exhibit varied activation thresholds across species (Laursen et al., 2015). The TRPA family has been divided into three major subfamilies, including TRPA1, TRPA1-like and 'basal' (also calls AsTRPA) (Himmel and Cox, 2020). Classical TRPA family members consists of 14 to 18 ankyrin repeat (ANK) domains at the N-terminal, six conserved transmembrane helical domains (S1-S6) and the C-terminal (Nilius and Owsianik, 2011). The ANK domains play a crucial role in the assembly, transportation, and thermal and chemical sensitivity of the TRPA1 channel (Cordero-Morales et al., 2011; Paulsen et al., 2015). TRPA1 is expressed in various tissues and cell types across different species, such as heart, nervous system, respiratory tract, pancreas, reproductive tissues, and muscles in mammals (Landini et al., 2022; Liu B. et al., 2022). TRPA1 is activated by a wide range of external stimuli, including thermal, cold, mechanical, various chemicals, and endogenous molecular signals (Logashina et al., 2019; Naert et al., 2020; Kashio and Tominaga, 2022). For example, TRPA1 in mammals was originally described as a noxious cold-activated channel (Story et al., 2003). It is further revealed that TRPA1 could function as a cold sensor, with heterologously expressed TRPA1 being activated by cold through mechanisms independent of Ca^{2+} influx and Ca^{2+} stores (Karashima et al., 2009). Additionally, recombinant human TRPA1 has been shown to be a versatile bidirectional thermal sensor, capable of detecting both cold and heat (Moparthy et al., 2016). Increasing evidence has demonstrated that TRPA1 participates in the inflammatory and immune responses in vertebrates (Talavera et al., 2020). TRPA1-mediated Ca^{2+} influx can modulate pro- or anti-apoptotic pathways and trigger neuronal apoptosis in the mouse oligodendrocytes (Sághy et al., 2016). Inhibiting TRPA1 has been shown to rectify the aberrant expression of apoptosis-associated proteins in rat chondrocytes (Yin et al., 2018), and reduced oxidative stress and apoptosis via UPR related pathways PERK/eIF2 α /ATF-4/CHOP signal in periodontal ligament cell (Liu Q. et al., 2022).

Compared to the extensive research in model animals, the research on TRPA1 in aquatic animals was much more limited, which mainly focused on the identification of TRPA1s and their expression profile under physiological properties (Stevens et al.,

2018; Lin et al., 2020; Li et al., 2023), mechanical pressure (Mahoney et al., 2011; Lin et al., 2020), chemical stress (Kozma et al., 2018; Kozma et al., 2020; Prober et al., 2008), and temperature stress (Oda et al., 2016; Saito et al., 2017; Oda et al., 2018; Ding et al., 2019; Li et al., 2019; de Alba et al., 2021; Peng et al., 2021; Liu B. et al., 2022; Li et al., 2023). TRPA1 activation in response to heat stimulation has been observed in various aquatic species, including zebrafish (*D. rerio*), pufferfish (*Takifugu*), crayfish (*Procambarus clarkii*), Zhikong scallop (*Chlamys farreri*), and starfish (*Patiria pectinifera*) (Oda et al., 2016; Saito et al., 2017; Oda et al., 2018; Li et al., 2019; Peng et al., 2021; Liu B. et al., 2022). Specifically, *Pc*TRPA expression was induced by high temperature (32°C), but not by low temperature (10°C) (Li et al., 2019; Liu B. et al., 2022). Zebrafish (*D. rerio*) zTRPA1b demonstrates a unique dual sensitivity, responding to both low and high temperature stimuli (Oda et al., 2016, 2018). The TRPA1 in Chinese mitten crab *Eriocheir sinensis* was induced by low temperature and suppressed by high temperature, playing a crucial role in regulating temperature adaptation (Li et al., 2023). Though there are a considerable number of researches on the correlation between temperature and TRPA1 in aquatic animals, their involvement in thermo-sensing and subsequent regulation of UPR and apoptosis remains unknown.

The Yesso scallop *Patinopecten yessoensis*, one of the dominant mariculture bivalve in the North Yellow Sea of China, is a cold-water species with the optimum growth temperature of 10-15°C (Li et al., 2007). Recently, the high temperature stress in summer has caused imbalance of energy homeostasis in cultured molluscs, which eventually results in large-scale mortalities. Timely sensing various stressors and triggering signaling pathways to induce the transcription of a variety of immune effectors may one of the important adaptation mechanisms for scallop *P. yessoensis*. Considering the important role of TRPA1s in sensing temperature and regulating the calcium homeostasis, a TRPA1-like was identified from scallop *P. yessoensis* (*Py*TRPA1-like) in the present study with the objectives to (1) characterize its sequence and expression characteristics, (2) investigate its activation after TRPA1 activator AITC and high temperature treatments, and (3) explore its involvement in regulating unfolded protein response (UPR) and apoptosis after TRPA1 antagonist HC-030031 and high temperature treatments.

2 Materials and methods

2.1 Scallops, treatments, and samples collection

Two-year-old Yesso scallops *P. yessoensis* with an average shell length of 6-8 cm were collected from a commercial farm in Dalian, China. The scallops were cultured in aerated seawater at 18°C and fed with diatom once a day for seven days before the following experiments. All experiments were performed in accordance with the approval and guidelines of the Ethics Review Committee of Dalian Ocean University.

Tissues including gill, gonad, hepatopancreas and mantle were collected from six scallops as six parallel samples, and haemolymph from these scallops was extracted and centrifuged at 800 × g, 4°C for 10 minutes to harvest the haemocytes. After addition of 1 mL Trizol reagent (Invitrogen), all the samples were stored at -80°C for RNA extraction.

One hundred and eight scallops were used for TRPA1 activator AITC (36682, Supelco) treatment experiment. These scallops were randomly divided into three groups including blank group, negative control group (DMSO group) and experiment group (AITC group). Scallops in negative control group and experiment group individually received an injection of 100 µL DMSO (10%, dissolved with PBS) and 100 µL AITC (20 mg/mL, dissolved with 10% DMSO) (Eid et al., 2008; Doihara et al., 2009). At 1 and 3 h after injection, haemocytes were collected from 18 scallops in each group to detect the mRNA expression of *PyTRPA1*-like, *PyGRP78*, *PyIRE1*, *PyATF6β*, *PyPERK* and *PyCaspase-3*, calcium content and distribution. At each point of time, three individuals in each group were randomly sampled and pooled as one sample, and six samples were conducted for each assay (N = 6).

Ninety scallops were used for high temperature stress experiment. They were firstly cultured in aerated seawater at 18°C (blank group, Blank) for seven days, and then 72 scallops were transferred to the seawater at 25°C for 1, 3, 6 and 12 h (high temperature stress treatment group, HT). Haemocytes were collected from 18 scallops in each group for follow-up testing the mRNA expression of *PyTRPA1*-like, *PyGRP78*, *PyIRE1*, *PyATF6β*, *PyPERK* and *PyCaspase-3*, the content and distribution of calcium, the activity of Caspase-3 and apoptosis rate. At each sampling point, three individuals in each group were randomly sampled and pooled as one sample, with six samples for each assay (N = 6).

One hundred and eight scallops were used for TRPA1 antagonist HC-030031 (H4415, Sigma-Aldrich) combined with high temperature treatment experiment. These scallops were randomly divided into three groups including blank group, negative control group (DH group) and experiment group (HH group). Scallops in negative control group and experiment group individually received an injection of 200 µL DMSO (1%, dissolved with PBS) and 200 µL HC-030031 (0.1 mg/mL, dissolved with 1% DMSO) combined with high temperature treatment (Eid et al., 2008; Liu Q. et al., 2022). At 1 and 12 h after treatment, haemocytes were collected from 18 scallops in each group to detect the mRNA expression of *PyTRPA1*-like, *PyGRP78*, *PyIRE1*, *PyATF6β*, *PyPERK* and *PyCaspase-3*, the content and distribution of calcium, the activity of Caspase-3 and apoptosis rate. At each point of time, three individuals in each group were randomly sampled and pooled as one sample, with six samples for each assay (N = 6).

2.2 Sequence analysis of *PyTRPA1*-like

The conserved domains of *PyTRPA1*-like were predicted using the simple modular architecture research tool (SMART) (<http://smart.embl-heidelberg.de/>). The amino acid sequence analyses and multiple sequence alignment were carried out using the BLAST

algorithm (<http://www.ncbi.nlm.nih.gov/BLAST>) and DNAMAN program, respectively. The neighbor-joining (NJ) phylogenetic tree of *PyTRPA1*-like was constructed using MEGA 7.0 software. Bootstrap trials were replicated 1000 times to derive the confidence value for phylogeny analysis (Tamura et al., 2007). The sequence information of TRPA1 proteins were described in Table 1, Supplementary Tables S1 and S2.

2.3 Analysis of mRNA expression using quantitative reverse transcription PCR (qRT-PCR)

Total RNA isolation and cDNA synthesis were performed according to previous reports (Wang et al., 2016). The SYBR Green qRT-PCR was carried out on an ABI 7500 Real-time Thermal Cycler platform according to the manufacturer's protocol (TaKaRa). All primers used in this assay were listed in Table 2. The *PyEF-α* gene (GenBank accession No. NW_018406511.1) was employed as internal control, and the relative expression level of *PyTRPA1*-like (XM_021509338.1), glucose-regulated protein 78 (*PyGRP78*, MF318508.1), inositol-requiring protein 1 (*PyIRE1*, MF318507.1), cyclic AMP-

TABLE 1 Sequences used for *PyTRPA1*-like alignment and phylogenetic analysis.

Protein name	Organism	Accession number
TRPA1	<i>Homo sapiens</i>	NP_015628.2
TRPA1	<i>Mus musculus</i>	NP_001335217.1
TRPA1	<i>Gallus gallus</i>	NP_001305389.1
TRPA1	<i>Drosophila melanogaster</i>	NP_001261602.1
TRPA1	<i>Xenopus tropicalis</i>	NP_001121434.1
TRPA1	<i>Anolis carolinensis</i>	NP_001280042.1
TRPA1a	<i>Danio rerio</i>	NP_001007066.1
TRPA1b	<i>Danio rerio</i>	NP_001007067.1
TRPA1b	<i>Takifugu rubripes</i>	XP_029699030.1
TRPA1b	<i>Oreochromis niloticus</i>	XP_025766241.1
TRPA1	<i>Sepia pharaonis</i>	CAE1328150.1
TRPA1-like	<i>Procambarus clarkii</i>	XP_045585225.1
TRPA1-like	<i>Eriocheir sinensis</i>	XP_050710403.1
TRPA1-like	<i>Penaeus japonicus</i>	XP_042871223.1
TRPA1	<i>Patiria pectinifera</i>	BAX76612.1
TRPA1-like	<i>Strongylocentrotus purpuratus</i>	XP_030839506.1
TRPA1	<i>Crassostrea gigas</i>	XP_034311437.1
TRPA1-like	<i>Crassostrea virginica</i>	XP_022317392.1
TRPA1-like	<i>Pecten maximus</i>	XP_033737357.1
TRPA1-like	<i>Patinopecten yessoensis</i>	XP_021365013.1

TABLE 2 Sequences of the primers used in the test.

Primer name	Primer sequence (5'-3')
PyTRPA1-like-RT-F	AACAGCCCTCCATGTTGCTTC
PyTRPA1-like-RT-R	TCCTGGGCTTCTATTGCGG
PyGRP78-RT-F	TCAGGGCAAGTGGAAGTAGC
PyGRP78-RT-R	GGTGACGTTCTGCTTAAC
PyIRE1-RT-F	AGCCAGTTCAGATGGCATGA
PyIRE1-RT-R	ACTTTCGCTTGACCTCACTTG
PyPERK-RT-F	AAAGGCGATGTCAGTCGTGT
PyPERK-RT-R	GGTCTCTCGGTTTGCCATGA
PyATF6 β -RT-F	TCCAGCCGCCCTGTACAAC
PyATF6 β -RT-R	TTCATCTCGTGGTCCACCTGC
PyCaspase-3-RT-F	AAGAGGCAGCTGGTTCATCC
PyCaspase-3-RT-R	ATCGGAGATTCCGACCACTC
Py EF- α -RT-F	GCGGTGGTATTGACAAGAGA
Py EF- α -RT-R	GTTCACGTTGAGCCTTCAGT

dependent transcription factor ATF-6 beta-like (PyATF6 β , XM_021519588.1), eukaryotic translation initiation factor 2-alpha kinase 3-like (PyPERK, XM_021518916.1) and caspase-3-like (PyCaspase-3, XM_021490863.1) were analyzed using the comparative Ct method ($2^{-\Delta\Delta C_t}$ method) (Wagner, 2013; Jia et al., 2015).

2.4 Determination of calcium content and distribution

2.4.1 Colorimetric assay of calcium content

The calcium content was measured according to the manufacturer's instructions of the calcium colorimetric assay kit (S1063S, Beyotime) (Zhao et al., 2021; Zhang et al., 2023). After haemocytes were obtained by centrifugation, an appropriate amount of lysate (about one million cells were resuspended in 200 μ L cell lysis buffer) was added. After adequate lysis of the haemocytes, the cell lysate was centrifuged at 14,000 \times g, 4°C for 5 min, and the supernatant was collected for determination (Zhang et al., 2023). A total of 50 μ L standard or sample and 150 μ L assay working solution were added into each well in 96-well microplate and incubated at room temperature for 10 min in the dark. The absorbance was re-corded by Infinite M1000 PRO (TECAN) at a wave length of 575 nm, and plot the standard curve.

2.4.2 Cellular calcium imaging

Cellular calcium imaging was carried out to investigate the intracellular distribution of calcium in haemocytes using the Fluo-4 calcium assay kit (S1061S, Beyotime) as previously described with some modification (Yu et al., 2021). The calcium content detection was performed according to previous reports and the operating instructions of the Fluo-4 calcium assay kit. The haemocytes were

collected with anticoagulant (510 mM NaCl, 200 mM glucose, 200 mM citric acid, 30 mM sodium citrate, 10 mM EDTA 2Na, pH 7.4) at the ratio of 1:1, and then centrifuged at 309 \times g, 4°C for 5 min immediately. The collected haemocytes were deposited onto poly-lysine coated glass slide for 1 h, incubated in 1 \times Fluo-4 staining solution at 37°C for 30 min and washed with PBS three times for one minute each time. After washing with PBS, the haemocytes on the glass slides were blocked with 1% BSA (40 min, 37°C) and washed with PBS three times. Haemocytes were incubated with PBS for 20 min at 37°C, followed by the nucleus was stained with DAPI (C1002, Beyotime, diluted at 1:1,000 (v/v) with 1% BSA) at room temperature for 15 min and washed by PBS for three times in the dark (Qin et al., 2014). The treated slides were stored at antifade mounting medium (P0126, Beyotime) and observed under inverted Laser Scan Confocal Microscope (ZEISS).

2.5 Analysis of Caspase-3 activity and apoptosis rate

2.5.1 Analysis of Caspase-3 activity

The Caspase-3 activity of hemocytes from blank group, HT group, negative control group (DH) and experiment group (HH) were detected using Caspase-3 Activity Assay Kit (C1116, Beyotime) according to previous description (Wu et al., 2016). The Caspase-3 activity detection were performed according to previous reports (Wu et al., 2018). Briefly, the haemocytes were collected as mentioned above, and resuspended in cell lysis buffer (about two million cells were resuspended in 100 μ L cell lysis buffer). The cell lysates were centrifuged at 20,000 \times g to collect the supernatant. The protein concentration for each sample was determined using Bradford kit. A total of 50 μ L cell lysate, 40 μ L assay buffer and 10 μ L AcDEVD-pNA (caspase-3 substrate) were added to each well in 96-well microplate and incubated at 37°C for 12 h. The absorbance was re-corded by Infinite M1000 PRO (TECAN) at a wave length of 405 nm. Cell lysis buffer instead of cell lysate was employed as control (Wu et al., 2018). All the samples were in six replicates.

2.5.2 Flow cytometric analysis

Haemolymph was collected with anticoagulant mixed solution with L15 (the ratio of 1:1) at the ratio of 1:1, and then centrifuged at 309 \times g, 4°C for 5 min immediately. The apoptosis rate was measured by Annexin V-FITC apoptosis detection kit (C1062L, Beyotime) according to manufacturer's instruction (Ge et al., 2020). The collected haemocytes were washed twice with anticoagulant mixed solution with L15, gently re-suspended in MAS mixed solution with L15 medium at a final concentration of $5 \times 10^5 - 1 \times 10^6$ cells·mL⁻¹ for the following experiment. Then 195 μ L Annexin V-FITC binding solution was added to the cell suspension and gently resuspended Haemocytes suspension was mixed thoroughly with 5 μ L Annexin V-FITC in the dark at room temperature for 25 min. Haemocytes were harvested by centrifugation at 309 \times g, 4°C for 5 min, resuspended in 500 μ L anticoagulant mixed solution with L15 medium, and then incubated with 10 μ L propidium iodide (PI)

for 5 min. After washing with anticoagulant mixed solution with L15 medium three times, the apoptosis rate of haemocytes in each group was analyzed by flow cytometer (BD Biosciences, USA). All the samples were in six replicates.

2.6 Statistical analysis

All data were analyzed using one-way analysis of variance (ANOVA). The results were given as mean ± S.D (n ≥ 4), and statistically significant difference was designated at *p* < 0.05.

3 Results

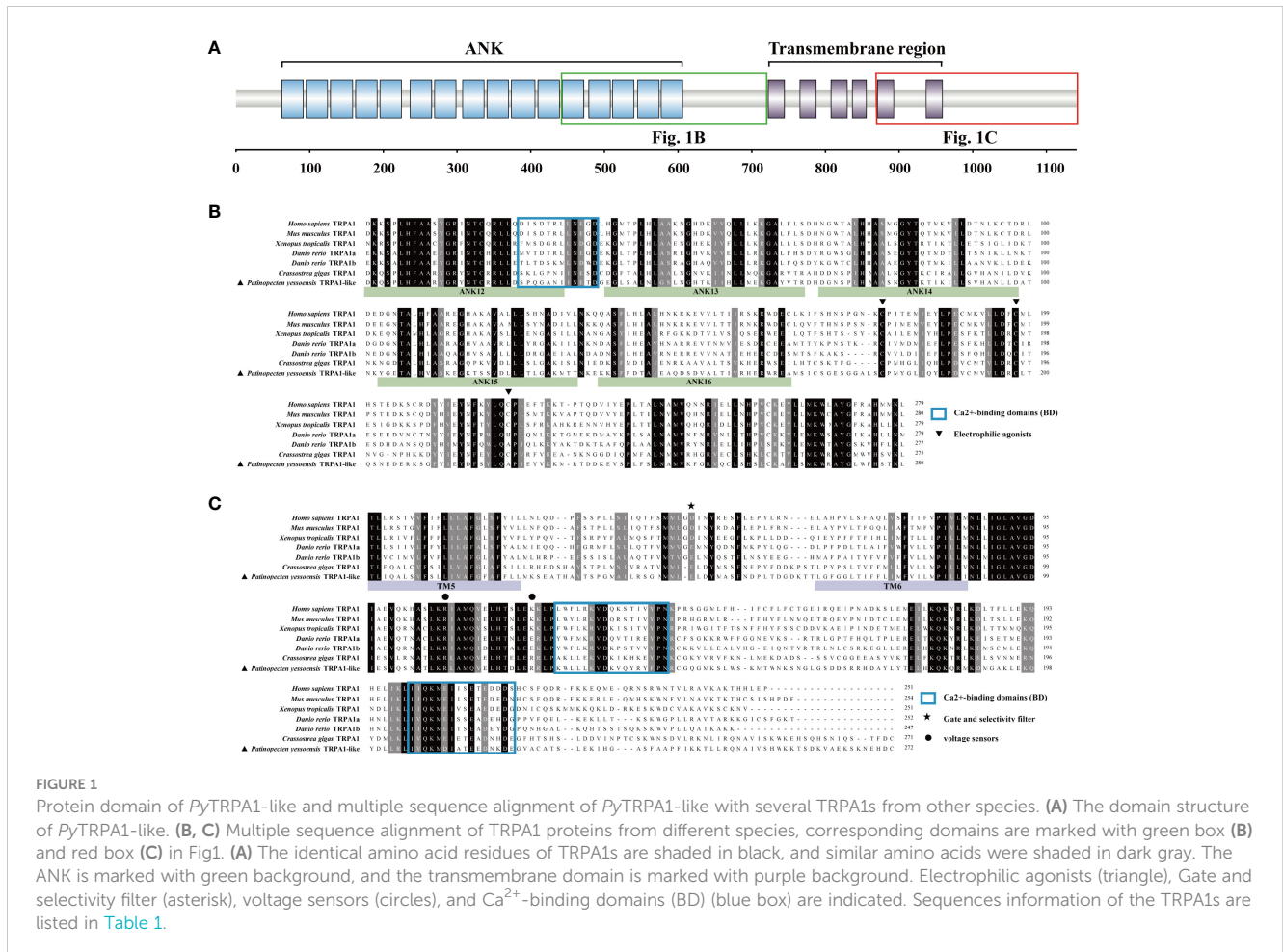
3.1 Molecular characteristics, phylogenetic evolution, and tissue distributions of PyTRPA1-like

The open reading frame (ORF) of PyTRPA1-like was of 3426 bp, encoding a polypeptide of 1141 amino acid residues with an isoelectric point of 6.51 and a molecular weight of 128 kDa. There were sixteen typical ANK domains and six transmembrane domains identified in PyTRPA1-like (Figure 1A). The presence of certain

functional sites observed in mammalian TRPA1s is also evident in PyTRPA1-like. Some residues, such as Cys620, Cys640, and Ala664 (usually referred to as Cys621, Cys641, and Cys665 in *Homo sapiens* TRPA1, were also observed in PyTRPA1-like, although the numbering varies in different species and isoforms) (Figure 1B). Two residues Arg980 and Arg993 (usually referred to as Arg975 and Lys989 in *H. sapiens* TRPA1) were found at the proximal portion of the COOH-terminus (Figure 1C). The outer gate of PyTRPA1-like is composed of diagonally opposed Glu917 (Asp915 residues in *H. sapiens*) (Figure 1C). The NH₂ tail and COOH-tail of PyTRPA1-like contain three putative Ca²⁺-binding domains (Figures 1B, C).

Multiple sequence alignment revealed that PyTRPA1-like shared low similarity with TRPA1s from *H. sapiens* (NP_015628.2, 32.44%), *Mus musculus* (NP_001335217.1, 31.21%), tropical clawed frog *Xenopus tropicalis* (NP_001121434.1, 32.84%), *Danio rerio* TRPA1a (NP_001007066.1, 33.82%), *D. rerio* TRPA1b (NP_001007067.1, 33.50%) (Supplementary Figure S1). PyTRPA1-like shared relatively higher similarity with TRPA1 from *Crassostrea gigas* (XP_034311437.1, 52.73%) (Supplementary Figure S1). The conserved value of the ANK domains and transmembrane domains range from 33.16%–58.51% and 26.01%–47.25%, respectively (Supplementary Figure S1).

A phylogenetic tree for different TRP subfamily genes from *H. sapiens*, *Mus musculus*, king scallop *Pecten maximus* and *P.*



yessoensis was firstly constructed. *PyTRPA1* was clearly clustered with TRPA1s (*P. maximus* TRPA1-like, *H. sapiens* TRPA1 and *M. musculus* TRPA1) (Supplementary Figure S2). Then, a phylogenetic tree for 36 TRPAs from different species was established to analyze the phylogenetic evolution of *PyTRPA1*-like. *PyTRPA1*-like was clustered with TRPA1s and TRPA1-like from invertebrates and vertebrates, showed relatively far evolutionary relationships with TRPA1-homolog, painless, pyrexia, water witch, TRPA5 and HsTRPA (Supplementary Figure S3). Finally, a phylogenetic tree for 13 TRPA1s and 7 TRPA1-likes from different species was further established to analyze the phylogenetic evolution of *PyTRPA1*-like. *PyTRPA1*-like and other eighteen TRPA family members were assigned into two major clades, invertebrate and vertebrate clade. *PyTRPA1*-like was firstly clustered with TRPA1s and TRPA1-likes from other molluscs (*P. maximus* TRPA1-like, *Crassostrea virginica* TRPA1-like, *C. gigas* TRPA1 and *Sepia pharaonic* TRPA1), then gathered with the TRPA1s and TRPA1-likes from the arthropods (*Penaeus japonicus* TRPA1-like, *E. sinensis* TRPA1-like, *P. sclarkii* TRPA1-like and *Drosophila melanogaster* TRPA1) and echinodermata (*P. pectinifera* TRPA1 and *Strongylocentrotus purpuratus* TRPA1-like), and finally clustered with TRPA1s from vertebrates (*H. sapiens* TRPA1, *M. musculus* TRPA1, *Gallus gallus* TRPA1, *Anolis carolinensis* TRPA1, *X. tropicalis* TRPA1, *D. rerio* TRPA1a, *D. rerio* TRPA1b, *Oreochromis niloticus* TRPA1b and *Takifugu rubripes* TRPA1b) (Figure 2A).

The transcripts of *PyTRPA1*-like were detected in haemocytes and all the examined tissues, including gill, mantle, gonad, adductor muscle and hepatopancreas. The highest mRNA expression level of *PyTRPA1*-like was detected in mantle, which was 475.73-fold of that in the haemocytes ($p < 0.05$) (Figure 2B). The expression level of *PyTRPA1*-like mRNA in hepatopancreas was also significantly higher than that in haemocytes (140.34-fold of that in the haemocytes, $p < 0.05$) (Figure 2B).

3.2 The temporal change of *PyTRPA1*-like mRNA, Ca^{2+} content and distribution after AITC treatment

The activation of *PyTRPA1*-like in haemocytes after TRPA1 activator AITC treatment was assessed by evaluating the relative expression level of *PyTRPA1*-like mRNA. At 3 h after AITC treatment, the relative expression level of *PyTRPA1*-like mRNA was significantly increased, which was 3.11-fold of that in the DMSO group ($p < 0.05$) (Figure 3A). However, there was no significant difference between the AITC group and the DMSO group at 1 h after treatment (Figure 3A). In contrast, the relative expression level of *PyTRPA1*-like mRNA in the DMSO group decreased significantly at 3 h (0.57-fold of that at 1 h, $p < 0.05$), while that in the blank group increased significantly at 3 h (1.66-fold of that at 1 h, $p < 0.05$) (Figure 3A).

The relative intracellular Ca^{2+} content in haemocytes of scallops after AITC treatment was determined by colorimetric assay. At 1 h and 3 h after AITC treatment, the Ca^{2+} content in haemocytes was significantly increased, which was 1.21-fold and 1.65-fold of that in the DMSO group ($p < 0.05$), respectively (Figure 3B). The Ca^{2+} content increased significantly at 3 h after AITC treatment (1.54-fold of that at 1 h, $p < 0.05$) (Figure 3B).

The cellular calcium imaging was used to detect the intracellular calcium distribution in scallop haemocytes at 3 h after AITC treatment. The morphology of the haemocytes was observed in a bright field, and the nucleus stained by DAPI was shown in blue fluorescence. The positive signals of Ca^{2+} labeled by Fluo-4 AM were indicated in green fluorescence. The positive signals of Ca^{2+} (marked green) show aggregated distribution in the cytoplasm of haemocytes in untreated scallops (Figure 3C). At 3 h after AITC treatment, the positive signals of Ca^{2+} were in dispersed distribution in the cytoplasm, and the overall fluorescence signal in haemocytes was significantly increased, compared to the DMSO group (Figure 3C).

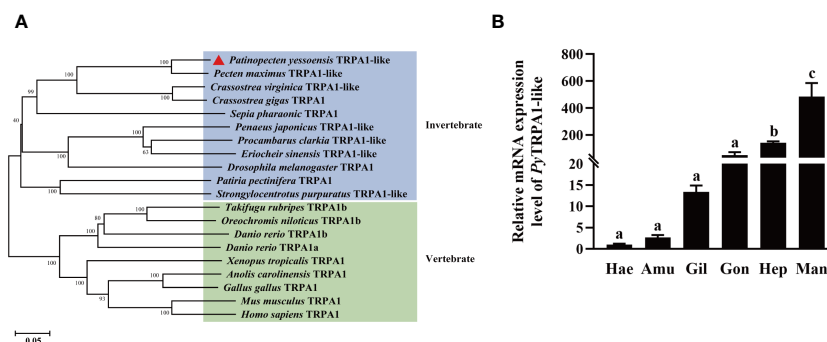


FIGURE 2

Phylogenetic evolution and tissue distributions of *PyTRPA1*-like. (A) Phylogenetic analysis of TRPA1s. The *PyTRPA1*-like was marked with a triangle. Sequence information of the eleven TRPA1s were described in Table 2. (B) The distribution of *PyTRPA1*-like mRNA in haemocytes and different tissues. Hae, haemocytes. Amu, adductor muscle. Gil, gill. Gon, gonad. Hep, hepatopancreas. Man, mantle. The relative mRNA expression level of *PyTRPA1*-like in different tissues and haemocytes was normalized to that of *PyEF- α* , and the significant difference is indicated by different letters. Each value was shown as mean \pm S.D. ($N \geq 4$).

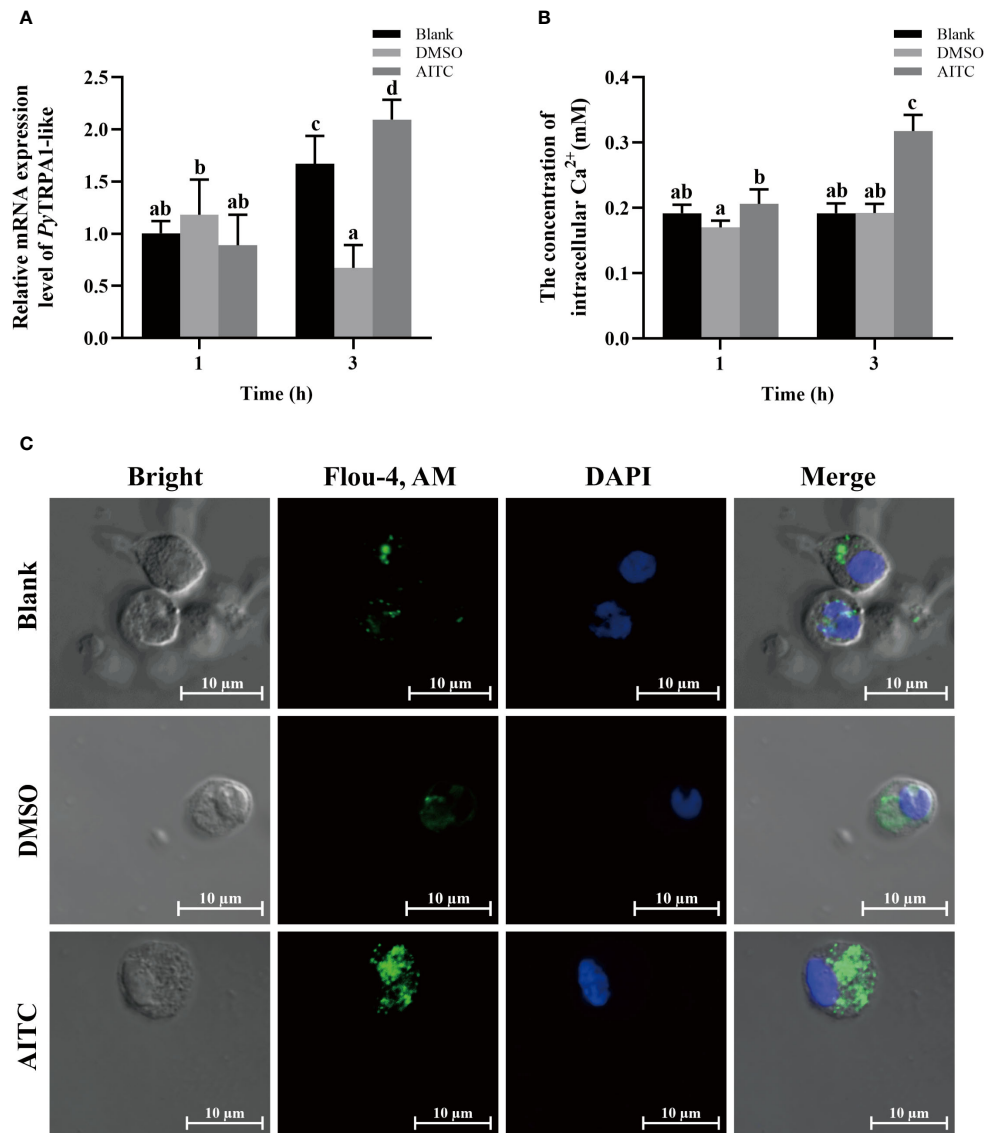


FIGURE 3

The temporal change of *PyTRPA1*-like mRNA, Ca^{2+} content and distribution in scallop haemocytes after AITC treatment. Blank, blank group. DMSO, scallops injection of 100 μL 10% DMSO. AITC, scallops injection of 100 μL 20 mg/mL AITC. (A) The relative expression level of *PyTRPA1*-like mRNA. (B) The relative intracellular Ca^{2+} content. (C) The intracellular calcium distribution of haemocytes. The significant difference was indicated by different letters. Each value is shown as mean \pm S.D. (N \geq 4).

3.3 The mRNA expression of UPR and apoptosis related genes after AITC treatment

The temporal mRNA expressions of UPR and apoptosis related genes in haemocytes after AITC treatment were investigated using qRT-PCR. At 3 h after AITC treatment, the relative expression levels of *PyGRP78*, *PyATF6 β* , *PyPERK* and *PyCaspase-3* mRNA increased significantly, which were 1.64-fold, 2.06-fold, 2.85-fold and 1.58-fold of that at 1 h ($p < 0.05$), respectively (Figures 4A, C-E). Specifically, the relative expression levels of *PyGRP78*, *PyPERK* and *PyCaspase-3* mRNA respectively were 1.60-fold, 5.06-fold and 1.67-fold of that in

the DMSO group ($p > 0.05$) (Figures 4A, D, E), however, that of *PyATF6 β* mRNA showed no significant difference compared with DMSO group (Figure 4C). At 1 h after AITC treatment, the relative expression level of *PyPERK* mRNA decreased significantly (0.44-fold of that in the DMSO group, $p < 0.05$) (Figure 4D), however, those of *PyGRP78*, *PyATF6 β* and *PyCaspase-3* mRNA showed no significant difference compared with DMSO group (Figures 4A, C, E). In contrast, the relative expression level of *PyIRE1* mRNA increased significantly at 1 h (2.36-fold of that in the DMSO group, $p < 0.05$). While that was significantly decreased at 3 h (0.73-fold of that at 1 h, $p < 0.05$), and there was no significant difference compared with DMSO group (Figure 4B).

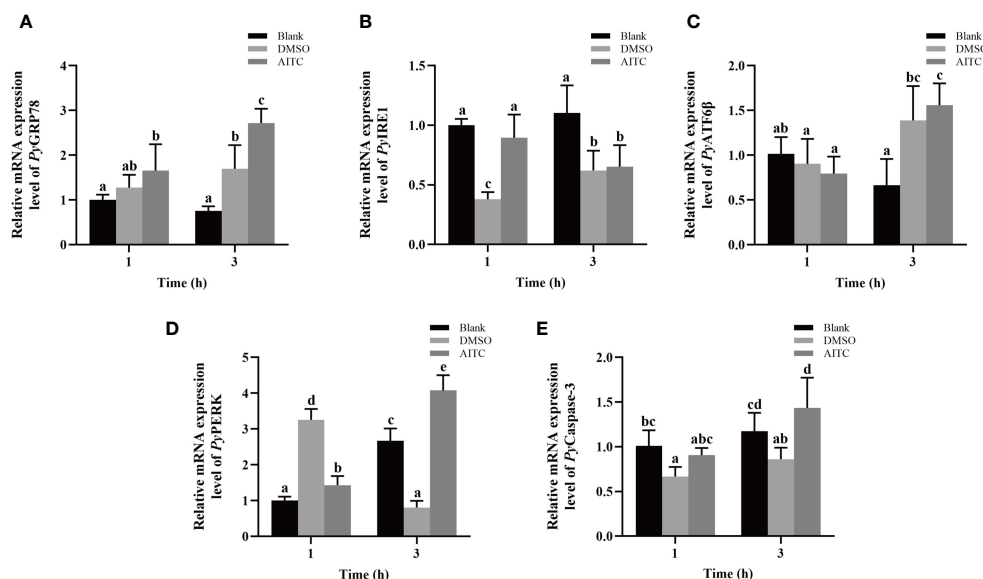


FIGURE 4

The mRNA expression of UPR and apoptosis related genes in scallop haemocytes after AITC treatment. Blank, blank group. DMSO, scallops injection of 100 μ L 10% DMSO. AITC, scallops injection of 100 μ L 20 mg/mL AITC. The relative mRNA expression level of UPR related genes *PyGRP78* (A), *PyIRE1* (B), *PyATF6 β* (C), and *PyPERK* (D), and apoptosis gene *PyCaspase3* (E). The significant difference is indicated by different letters. Each value was shown as mean \pm S.D. (N \geq 4).

3.4 Changes of *PyTRPA1*-like mRNA, Ca^{2+} content and distribution after high temperature treatment

The relative expression level of *PyTRPA1*-like mRNA in haemocytes after high temperature treatment (25°C) was investigated using qRT-PCR. After high temperature treatment, the relative expression level of *PyTRPA1*-like mRNA was significantly upregulated at 3 h (16.18-fold of that in the blank group, $p < 0.05$), reached the peak level at 6 h (85.45-fold of that in the blank group, $p < 0.05$), and dropped back to normal level at 12 h (Figure 5A).

The relative intracellular Ca^{2+} content in haemocytes of scallops after high temperature treatment was determined by colorimetric assay. After high temperature treatment, the relative intracellular Ca^{2+} content in haemocytes increased significantly and reached the peak level at 1 h (3.10-fold of that in the blank group, $p < 0.05$) (Figure 5B), remained significantly upregulated level at 3 h and 6 h ($p < 0.05$), and dropped back to normal level at 12 h ($p > 0.05$) (Figure 5B).

The cellular calcium imaging was used to detect the intracellular calcium distribution in scallop haemocytes after high temperature treatment. The morphology of the haemocytes was observed in a bright field, and the nucleus stained by DAPI was shown in blue fluorescence. The positive signals of Ca^{2+} labeled by Fluo-4 AM were indicated in green fluorescence. The positive signals of Ca^{2+} (marked green) show aggregated distribution in the cytoplasm of haemocytes in untreated scallops (Figure 5C). After high temperature treatment, the positive signals of Ca^{2+} were in dispersed distribution in the cytoplasm and the overall fluorescence signal in haemocytes increased significantly at 1 h

(Figure 5C), while the positive signals of Ca^{2+} recovered aggregated distribution in the cytoplasm and the overall fluorescence signal in haemocytes dropped back to normal level at 12 h (Figure 5C).

3.5 The mRNA expression of UPR related genes after high temperature treatment

The mRNA expressions of UPR related genes in haemocytes after high temperature treatment were investigated using qRT-PCR. After high temperature treatment, the relative expression levels of *PyGRP78*, *PyATF6 β* and *PyPERK* mRNA were quickly upregulated at 1 h, reached the peak level at 6 h (11.65-fold of that in the blank group, $p < 0.05$), 3 h (3.94-fold of that in the blank group, $p < 0.05$), respectively, and recovered to the blank level at 12 h ($p > 0.05$) (Figures 6A, C, D). In contrast, the relative expression level of *PyIRE1* mRNA decreased significantly at 1 h and 3 h (0.51-fold and 0.55-fold of that in the blank group, $p < 0.05$), then recovered to the normal level at 6 h ($p > 0.05$), and increased significantly at 12 h (1.67-fold of that in the blank group, $p < 0.05$) (Figure 6B).

3.6 Changes of *PyCaspase-3* mRNA expression, Caspase-3 activity, and apoptosis rate after high temperature treatment

To explore the effect of high temperature stress on apoptosis, *PyCaspase-3* mRNA expression, Caspase-3 activity, and apoptosis rate in hemocytes were detected after high temperature

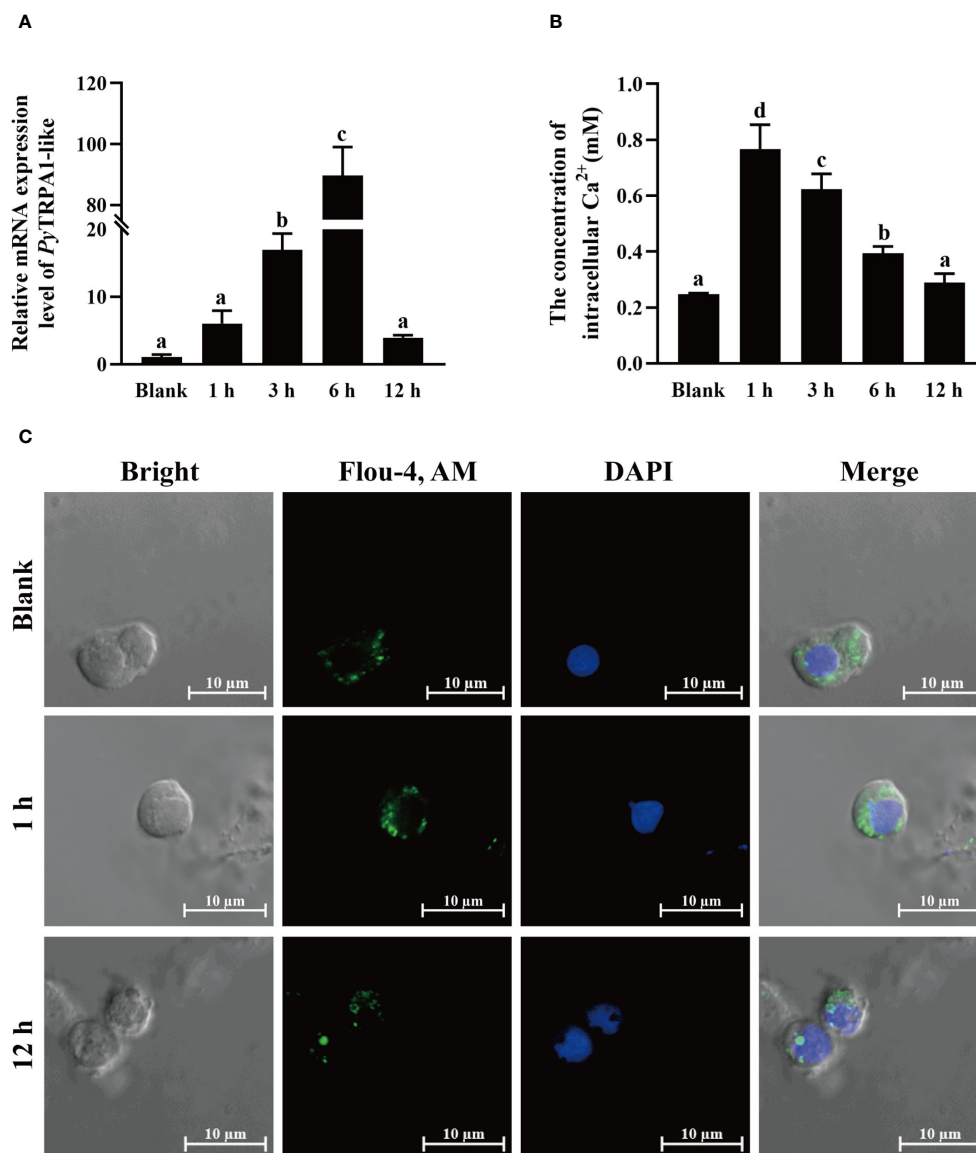


FIGURE 5
The change of *PyTRPA1*-like mRNA, Ca²⁺ content and distribution in scallop haemocytes after high temperature treatment. **(A)** The relative expression level of *PyTRPA1*-like mRNA. **(B)** The relative intracellular Ca²⁺ content. **(C)** The intracellular calcium distribution in haemocytes. The significant difference is indicated by different letters. Each value is shown as mean \pm S.D. (N \geq 4).

treatment. The relative expression level of *PyCaspase-3* mRNA increased significantly at 3 h after treatment (1.48-fold of that in the blank group, $p < 0.05$), reached the highest level at 12 h (2.71-fold of that in the blank group, $p < 0.05$) (Figure 7A). At 12 h after high temperature treatment, the Caspase-3 activity increased significantly (1.79-fold of that in the blank group, $p < 0.05$), however, there was no significant difference at 6 h between the HT and blank group (Figure 7B). At 6 h and 12 h after high temperature treatment, the apoptosis of haemocytes was assessed by Annexin V-FITC and PI staining followed by analysis with flow cytometry (Figure 7C). The apoptosis rate of haemocytes at 6 h after high temperature treatment (8.33%) shown no significant difference with that in the blank group (10.55%) ($p > 0.05$) (Figure 7D), while

that increased significantly at 12 h after high temperature treatment (29.47%, 2.79-fold of that in the blank group, $p < 0.05$) (Figure 7D).

3.7 Changes of *PyTRPA1*-like mRNA, Ca²⁺ content and distribution after HC-030031 combined with high temperature treatment

The relative expression level of *PyTRPA1*-like mRNA in haemocytes after TRPA1 antagonist (HC-030031) combined with high temperature treatment (25°C) was investigated using qRT-PCR. The relative expression level of *PyTRPA1*-like mRNA

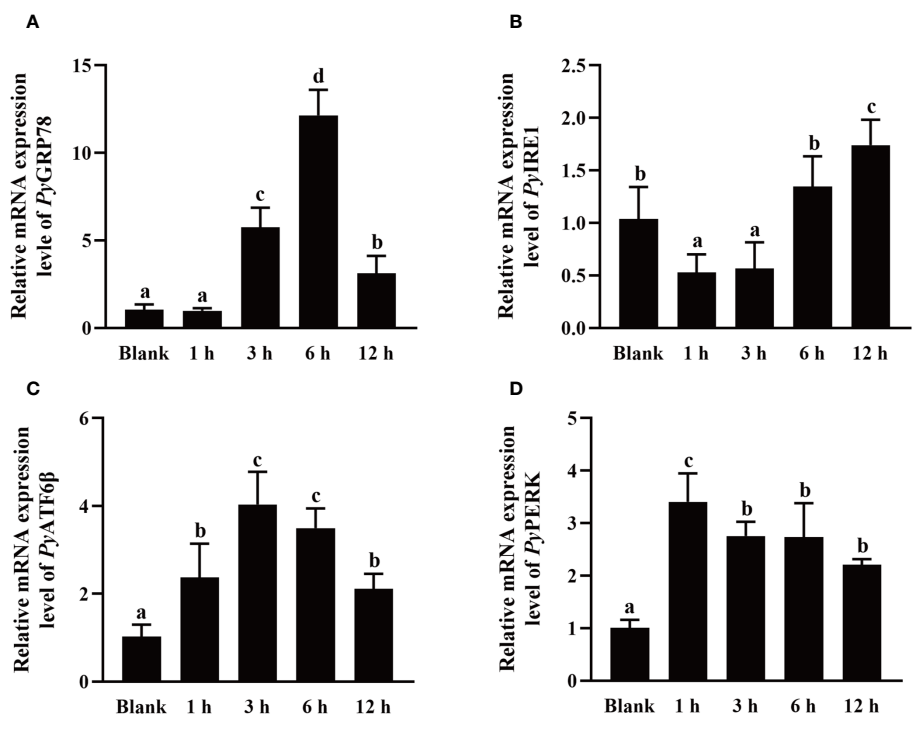


FIGURE 6 The mRNA expression of UPR related genes after high temperature treatment. The relative mRNA expression level of UPR related genes *PyGRP78* (A), *PyIRE1* (B), *PyATF6β* (C), and *PyPERK* (D). The significant difference is indicated by different letters. Each value is shown as mean ± S.D. (N ≥4).

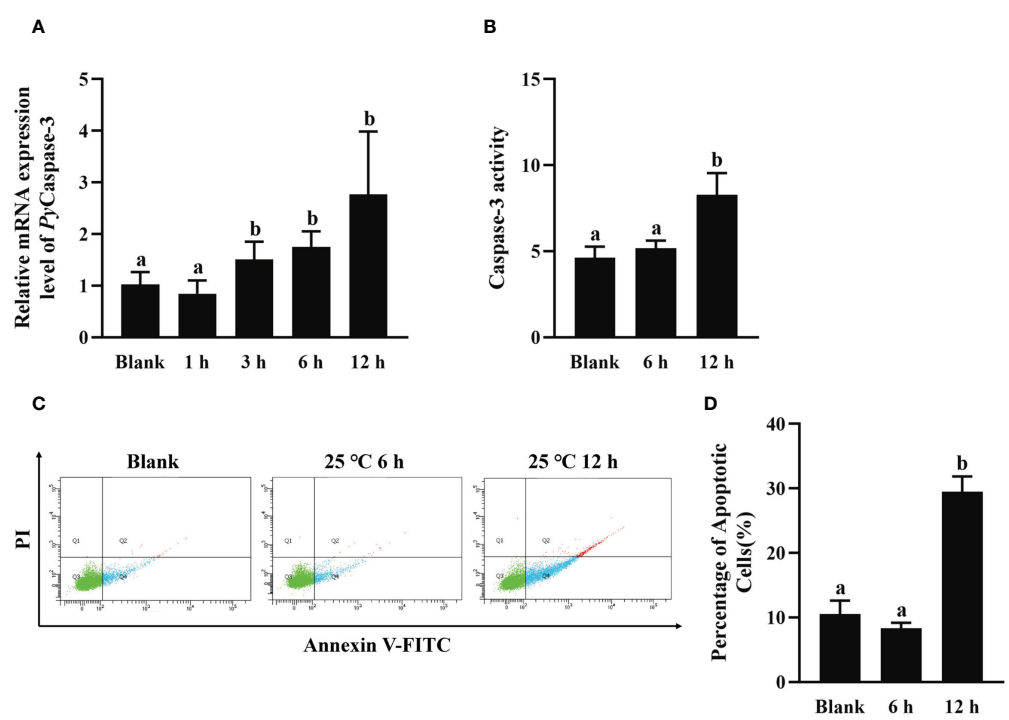


FIGURE 7 The change of *PyCaspase-3* mRNA expression, Caspase-3 activity and apoptosis rate after high temperature treatment. (A) The relative expression level of *PyCaspase-3* mRNA. (B) Caspase-3 activity. (C) The apoptotic haemocytetes detected by Annexin V-FITC/PI staining, and (D) The apoptosis rate of haemocytetes. The significant difference is indicated by different letters. Each value is shown as mean ± S.D. (N ≥4).

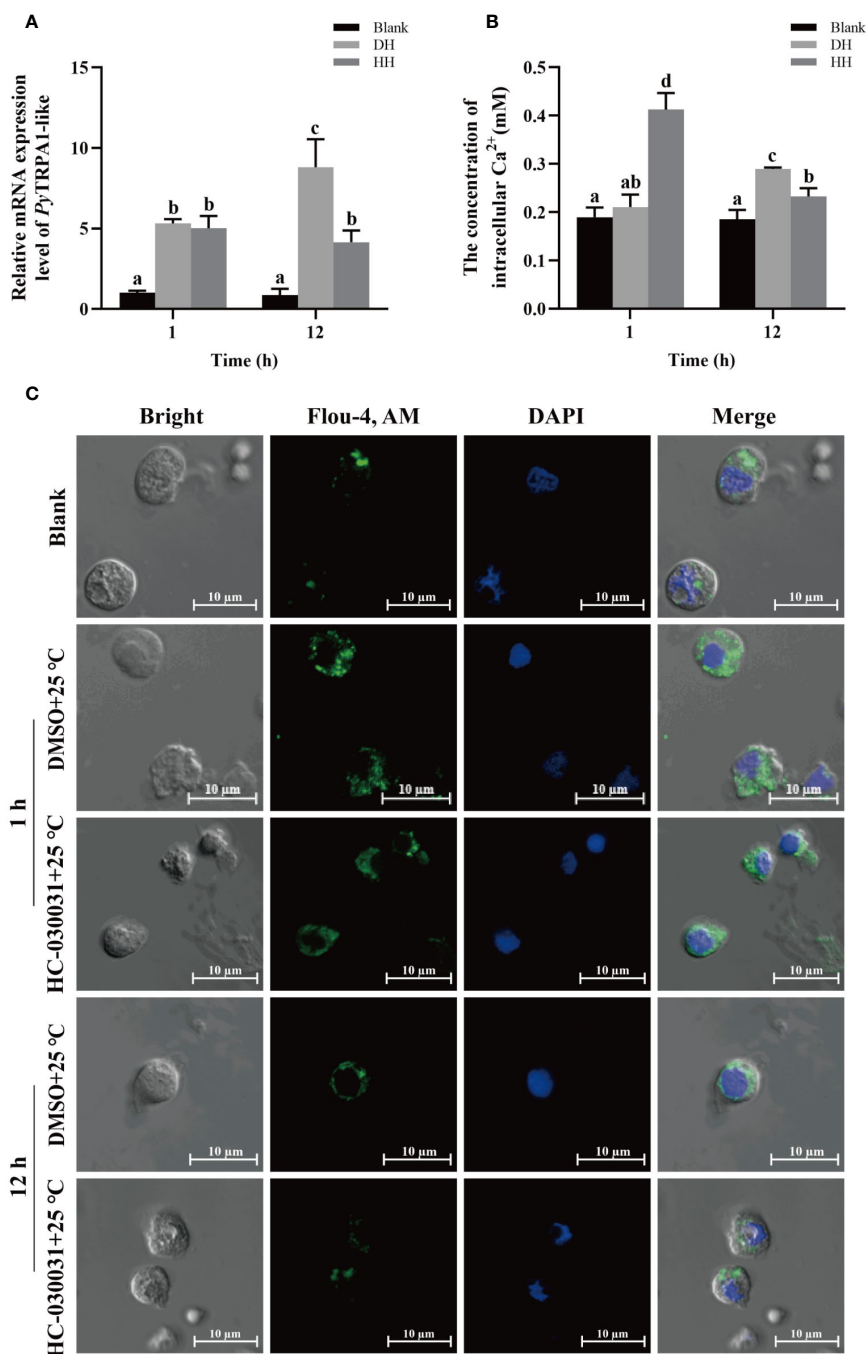


FIGURE 8

The temporal change of *PyTRPA1*-like mRNA, Ca^{2+} content and distribution in scallop haemocytes after HC-030031 combined with high temperature treatment. Blank, blank group. DH, scallops injection of 200 μL 1% DMSO combined with high temperature treatment. HH, scallops injection of 200 μL 0.1 mg/mL HC-030031 combined with high temperature treatment. (A) The relative expression level of *PyTRPA1*-like mRNA. (B) The relative content of intracellular Ca^{2+} . (C) The distribution of intracellular Ca^{2+} in haemocytes. The significant difference is indicated by different letters. Each value is shown as mean \pm S.D. (N \geq 4).

decreased significantly at 12 h after treatment (0.47-fold of that in the DH group, $p < 0.05$), however, there was no significant difference at 1 h between the HH and DH group (Figure 8A).

The relative intracellular Ca^{2+} content in haemocytes of scallops after HC-030031 combined with high temperature treatment was determined by colorimetric assay. At 1 h after treatment, the Ca^{2+} content in haemocytes increased significantly (1.96-fold of that in

the DH group, $p < 0.05$), while that decreased significantly at 12 h (0.56-fold of that at 1 h and 0.80-fold of that in the DH group, $p < 0.05$) (Figure 8B).

The intracellular calcium distribution in scallop haemocytes after HC-030031 combined with high temperature treatment was investigated. The positive signals of Ca^{2+} (marked green) show aggregated distribution in the cytoplasm of haemocytes in

untreated scallops (Figure 8C). At 1 h after HC-030031 combined with high temperature treatment, the positive signals of Ca^{2+} were dispersed distribution in the cytoplasm, and the overall fluorescence signals in haemocytes showed no significant difference compared with the DH group (Figure 8C). At 12 h after HC-030031 combined with high temperature treatment, the positive signals of Ca^{2+} recovered aggregated distribution in the cytoplasm, the overall fluorescence signal in haemocytes were significantly decreased compared with the DH group (Figure 8C).

3.8 The mRNA expression of UPR related genes after HC-030031 treatment and high temperature exposure

The relative mRNA expressions of UPR related genes in haemocytes after HC-030031 combined with high temperature treatment were investigated. The relative expression levels of *PyGRP78* and *PyIRE1* mRNA decreased significantly at 12 h (0.36-fold of that in the DH group, $p < 0.05$) and 1 h (0.29-fold of that in the DH group, $p < 0.05$), respectively (Figures 9A, B). The relative expression level of *PyGRP78* mRNA increased significantly at 1 h (4.54-fold of that in the DH group, $p < 0.05$) (Figure 9A), while there was no significant difference in the relative expression level of *PyIRE1* mRNA at 12 h between the HH and DH group

(Figure 9B). In contrast, the relative expression levels of *PyATF6 β* and *PyPERK* mRNA showed no significant difference at 1 h and 12 h between the HH and DH group (Figures 9C, D). Furthermore, the relative expression level of *PyGRP78*, *PyATF6 β* and *PyPERK* mRNA decreased significantly at 12 h, which were 0.36-fold, 0.29-fold and 0.17-fold of that at 1 h, respectively ($p < 0.05$) (Figures 9A, C, D), while the relative expression level of *PyIRE1* mRNA increased significantly (4.63-fold of that at 1 h, $p < 0.05$) (Figure 9B).

3.9 Changes of *PyCaspase-3* mRNA expression, Caspase-3 activity, and apoptosis rate after HC-030031 combined with high temperature treatment

To investigate the function of *PyTRPA1* in apoptosis, *PyCaspase-3* mRNA expression, Caspase-3 activity, and apoptosis rate in hemocytes were detected after HC-030031 combined with high temperature stress treatment. At 1 h after treatment, the relative expression level of *PyCaspase-3* mRNA increased significantly (3.98-fold of that in the DH group, $p < 0.05$), while that decreased significantly at 12 h (0.19-fold of that at 1 h and 0.16-fold of that in the DH group, $p < 0.05$) (Figure 10A). At 12 h after treatment, the Caspase-3 activity decreased significantly (0.65-fold of that in the DH group, $p < 0.05$) (Figure 10B). The apoptosis of

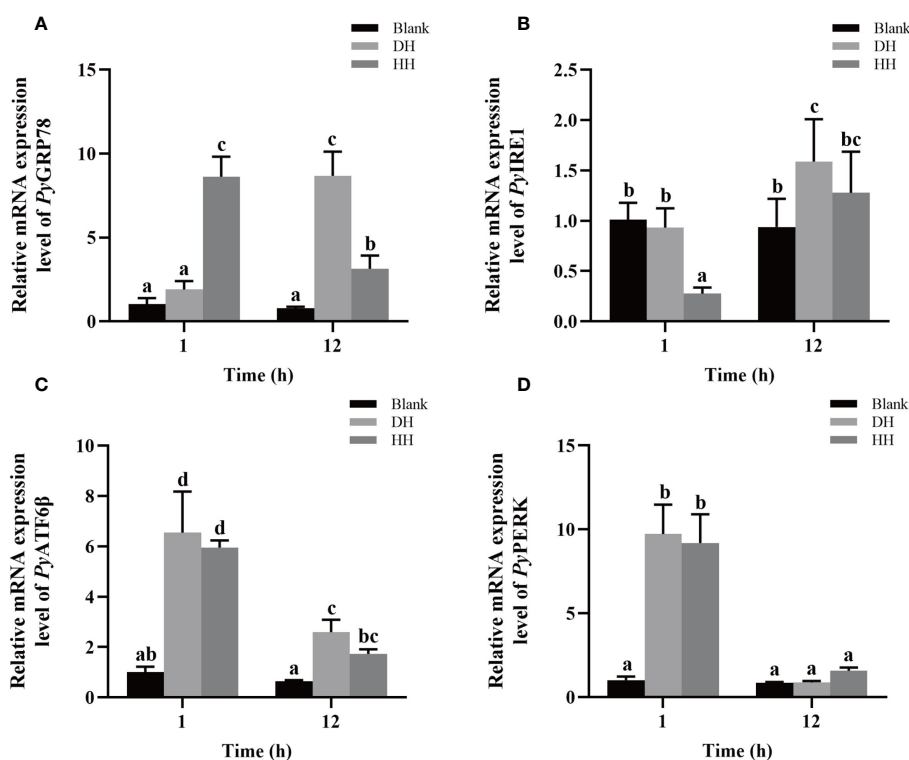


FIGURE 9

The mRNA expression of UPR related genes after HC-030031 combined with high temperature stress treatment. Blank, blank group. DH, scallops injection of 200 μL 1% DMSO combined with high temperature treatment. HH, scallops injection of 200 μL 0.1 mg/mL HC-030031 combined with high temperature treatment. The relative expression level of UPR related genes *PyGRP78* (A), *PyIRE1* (B), *PyATF6 β* (C), and *PyPERK* (D) mRNA. The significant difference was indicated by different letters. Each value was shown as mean \pm S.D. ($N \geq 4$).

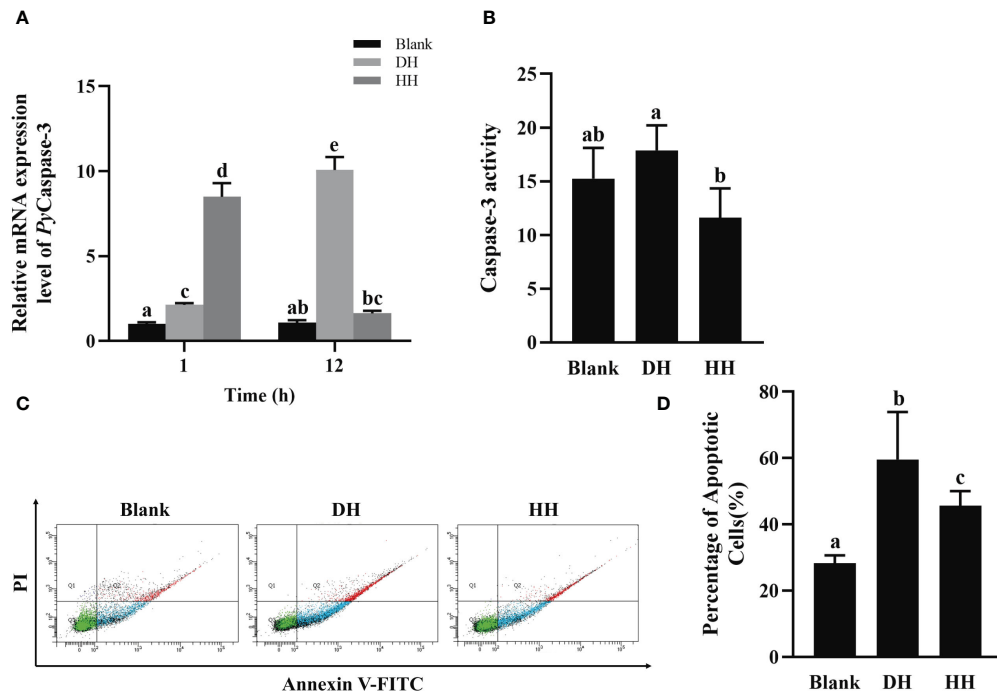


FIGURE 10

The temporal change of *PyCaspase-3* mRNA expression, Caspase-3 activity and apoptosis rate after HC-030031 combined with high temperature stress treatment. Blank, blank group. DH, scallops injection of 200 μ L 1% DMSO combined with high temperature stress treatment. HH, scallops injection of 200 μ L 0.1 mg/mL HC-030031 combined with high temperature stress treatment. (A) The relative expression level of *PyCaspase-3* mRNA. (B) Caspase-3 activity alteration at 12 h after treatment. (C) The apoptotic haemocytes were detected by Annexin V-FITC/PI staining at 12 h after treatment. (D) apoptosis rate. The significant difference is indicated by different letters. Each value is shown as mean \pm S.D. (N \geq 4).

haemocytes was assessed by Annexin V-FITC and PI staining followed by analysis with flow cytometry (Figure 10C). The apoptosis rate decreased significantly at 12 h after treatment (45.62% VS 59.57%, 0.77-fold of that in the DH group, $p < 0.05$) (Figure 10D).

4 Discussion

4.1 The structural and expression characteristics of *PyTRPA1*-like

Various studies have investigated the TRPA1 channel has 14 to 18 ankyrin repeat (ANK) domains and six transmembrane domains (Nilius and Owsianik, 2011). In the present study, there were sixteen typical ANK domains and six transmembrane domains identified in *PyTRPA1*-like, which was consistent with the classical TRPA1 in vertebrates (Nilius and Owsianik, 2011). Except for the typical domains and motifs, some other functional sites identified in mammalian TRPA1 are also observed in *PyTRPA1*-like, including two cysteine residues Cys620, Cys640, and an alanine residue Ala664 which are critical for TRPA1 activation by electrophilic agonists (Cordero-Morales et al., 2011; Paulsen et al., 2015), two arginine residues Arg980 and Arg993 which control the voltage-dependent activation of TRPA1 at highly depolarizing potentials ($>+100$ mV) (Samad et al., 2011), and one glutamate residue Glu917 which controls Ca^{2+} permeability (Paulsen et al., 2015). Moreover, there

were three putative Ca^{2+} -binding domains located in the NH_2 - and COOH-tail of *PyTRPA1*-like. These key functional sites of *PyTRPA1*-like exhibit a certain degree of conservation and variation with those in mammal (*H. sapiens* and *Mus musculus*) and aquatic animal TRPA1 (*D. rerio* and *C. gigas*), indicating that *PyTRPA1*-like can also engage in diversified functions similar to TRPA1s in other species (Doerner et al., 2007; Sura et al., 2012; Talavera et al., 2020). *PyTRPA1*-like was firstly clustered with TRPA1s from other molluscs, then gathered with the TRPA1s from the arthropods and echinodermata, and finally clustered with TRPA1s from vertebrates, indicating that molluscan TRPA1s shared closer evolutionary relationships with their invertebrate homologues. It has been demonstrated that TRPA1 genes are widely conserved from vertebrates to insects, and it is likely that TRPA1 is owned by heat sensitivity during the early stages of animal evolution (Saito et al., 2015; Sinica and Vlachová, 2021). All these results indicated that *PyTRPA1*-like shared structure conservation with its homologues in vertebrates.

It is reported that TRPA1 is broadly expressed in various tissues and a wide range of cells in different species (Li et al., 2019; Peng et al., 2021; Landini et al., 2022; Li et al., 2023). In the present study, *PyTRPA1*-like mRNA was constitutively expressed in haemocytes and a variety of tissues, and this wide distribution profile was also observed in other aquatic invertebrate, such as *P. clarkii* (Li et al., 2019; Peng et al., 2021) and *E. sinensis* (Li et al., 2023), suggesting that *PyTRPA1*-like might play an important role in various physiological processes. The structural and expression characteristics collectively

suggested that *PyTRPA1*-like might engage in diversified functions in scallop like its homologues in other species.

4.2 The activation of *PyTRPA1*-like by AITC and high temperature

Accumulating evidences have shown that TRPA1 is a polymodal ion channel sensitive to temperature and chemical stimuli (Laursen et al., 2015; Mahajan et al., 2021). However, compared to the vast knowledge on TRPs channel regulation, little is known about the induction mechanism of TRPs transcription (Nilius and Flockerzi, 2014). In the present study, the relative expression level of *PyTRPA1*-like mRNA were significantly upregulated after TRPA1 specific activator AITC and high temperature treatment, indicating that *PyTRPA1*-like was activated by AITC and high temperature. This is consistent with the previous study that AITC enhances TRPA1 activity by selectively targeting the active mercaptan groups of cysteine and lysine in the NH₂ terminal domain (Mahajan et al., 2021). Unlike the classical activation effect of AITC on those TRPA1 from both vertebrates and invertebrates (Doihara et al., 2009; Kurganov et al., 2014), there are some controversy on the functions of TRPA1 in temperature sensing. TRPA1 was initially identified as a cold activated channel (Story et al., 2003), and its activation by heat stimulation (and some non-mammalian vertebrates) was subsequently reported in invertebrates (Oda et al., 2016; Saito et al., 2017; Oda et al., 2018; Li et al., 2019; Peng et al., 2021), indicating that TRPA1 can function as both thermal and cold activated channels in different species (Buijs and McNaughton, 2020). The thermo-TRPA1 channels exhibit varied activation thresholds across species, suggesting evolutionary adaptations in TRPA1 temperature sensitivity to suit specific ecological niches (Laursen et al., 2015). The thermal activation of *PyTRPA1*-like was similar with that in Zhikong scallop *C. farreri* (Doihara et al., 2009; Kurganov et al., 2014) and crayfish *P. clarkia* (Li et al., 2019), while different from that in Chinese mitten crab *E. sinensis* (Oda et al., 2016, 2018), zebrafish *D. rerio* (Oda et al., 2016, 2018), and sea urchins *S. intermedius* (Ding et al., 2019). HC-030031, the specific TRPA1 antagonist, failed to show any inhibitory effects on western clawed frog *Xenopus tropicalis* fTRPA1 or zebrafish *D. rerio* zTRPA1b, whereas it showed dose-dependent inhibition of human TRPA1 activity (Gupta et al., 2016). In the present study, the relative expression of *PyTRPA1*-like mRNA in haemocytes were significantly down-regulated at 12 h after HC-030031 treatment, further indicating that the functional mechanism of TRPA1 in heating sensing may differ among species. In the following study, we will explore its biological effects under low temperature stress.

4.3 The regulation of *PyTRPA1*-like on Ca²⁺ content in cytoplasm

As a nonselective cation channel, TRPA1 exhibits a higher permeability to Ca²⁺ compared to other TRP channels (Nilius and

Owsianik, 2011; Nilius et al., 2012), and is able to be activated by multiple factors (Talavera et al., 2020). The rapid activation of TRPA1 in response to acute stimuli is triggered by local Ca²⁺ influx (Schmidt et al., 2009). In the present study, the Ca²⁺ content was significantly increased within 3 h after AITC treatment. Simultaneously, the positive signals of Ca²⁺ were dispersed distribution in the cytoplasm, and the overall fluorescence signal in haemocytes was also significantly increased, indicating that the calcium distribution in scallop haemocytes underwent alterations after the activation of TRPA1. The increased TRPA1 also contribute significantly to the disruption of intracellular calcium content (Liu Q. et al., 2022). The Ca²⁺ content in haemocytes increased significantly at 1 h after high temperature treatment, and then recovered to the normal level at 12 h. Simultaneously, the positive signals of Ca²⁺ were dispersed distribution in the cytoplasm, and the overall fluorescence signal in haemocytes was also significantly increased, then returned to the aggregated distribution at 12 h, indicating that the calcium distribution in scallop haemocytes underwent alterations and could subsequently be restored after high temperature treatment. The observed phenomenon may be attributed to the fact that the influx of Ca²⁺ can induce rapid channel inactivation, which may be triggered when the local cellular concentration of Ca²⁺ exceeds a certain threshold (Wang et al., 2008), which was consistent with the trend observed in relative expression level of *PyTRPA1*-like mRNA. After HC-030031 (TRPA1 antagonist) and high temperature stress treatment, the intracellular Ca²⁺ content decreased significantly and the Ca²⁺ distribution in haemocytes showed no difference with that in control group, suggesting that HC-030031 inhibited the intracellular Ca²⁺ content increased.

4.4 Effect of *PyTRPA1*-like on UPR and apoptosis after high temperature stress treatment

The ER protein maturation capacity may be overwhelmed due to the action of several cell intrinsic and extrinsic factors, causing ER stress (Santamaría et al., 2019). The accumulation of unfolded proteins triggers the activation of the three ER-resident sensors responsible for UPR by sequestering GRP78 (Santamaría et al., 2019). The activation of UPR signaling pathway during ER stress is mediated by three transmembrane sensors, including IRE1, PERK, and ATF6, which exert different activation and regulatory mechanisms (Bhardwaj et al., 2020). IRE1, the most conserved UPR pathway, could be activated by oligomerization and autophosphorylation (Shamu and Walter, 1996), induces degradation of membrane-associated mRNAs to reduce the level of nascent proteins (Tabas and Ron, 2011). ATF6 has an autocatalytic site, and cleaves its cytosolic bZIP domain that transcribes protein-folding chaperons to reduce the ER stress (Chiang et al., 2012). PERK receives the signal of aggregated misfolded proteins in ER lumen (Pandey et al., 2019), and induces the phosphorylation of ELF2 α which inhibits protein translation and induces apoptosis. To explore the regulation of

UPR after TRPA1 activation, the mRNA expressions of four UPR key genes were investigated. The expression level of *PyGRP78*, *PyIRE1*, *PyATF6 β* , and *PyPERK* mRNA in haemocytes were all significantly increased after TRPA1 specific activator AITC and high temperature treatment, indicating the UPR were activated by AITC and high temperature, which was consistent with the previous study (Lee, 2005; Wu et al., 2018; Liu et al., 2020; Yang et al., 2021). The relative expression levels of *PyGRP78* and *PyIRE1* mRNA in haemocytes shown significant up-regulations and the peak values appeared at a later time compared to that of *PyATF6 β* , and *PyPERK*. The different expression profiles of *PyIRE1*, *PyATF6 β* and *PyPERK* in the present study after AITC and high temperature treatment may due to their different activation and regulatory mechanisms in response to ER stress (Eletto et al., 2014; Ibrahim et al., 2019). All three ER stress sensors trigger downstream signalling pathways that control survival or death decisions (Santamaría et al., 2019). Increasing intracellular Ca^{2+} concentration induced by TRPA1 activation, which is always related with increased ER stress as well as cell apoptosis (Germande et al., 2022; Liu Q. et al., 2022). Our results demonstrated that the *PyCaspase-3* mRNA, Caspase-3 activity and apoptosis rate of haemocytes were significantly increased after AITC and high temperature treatment, similar to the previous observations (Yang et al., 2017; Liu et al., 2020). However, the underlying regulation mechanism of TRP in those primitive allotherm response upon temperature stress may be more complex than expected, which needs further investigation.

TRPA1 inhibitor significantly inhibit TRPA1, and decreased the intracellular calcium, then exerted anti-apoptotic functions in inflammatory periodontal ligament cell via inhibiting ER stress by downregulating UPR related pathways (Liu Q. et al., 2022). The results obtained in our study produced similar outcomes, after HC-030031 combined with high temperature stress treatment, the relative expression level of *PyGRP78*, *PyIRE1*, *PyATF6 β* , and *PyPERK* mRNA in haemocytes could be inhibited within 12 h, suggesting that significantly activated under high temperature stress and was significantly decreased by TRPA1 antagonist. The mRNA expression of the UPR key genes recovered to normal or low level from 12h after HC-030031 combined with high temperature stress treatment, indicating that there was a mechanism limiting UPR signaling and maintaining it within a physiologically appropriate range (Eletto et al., 2014). After HC-030031 combined with high temperature stress treatment, the mRNA expression level of *PyCaspase-3*, Caspase-3 activity and apoptosis rate in haemocytes could be inhibited within 12 h, suggesting that significantly increased under high temperature stress and was significantly decreased by TRPA1 antagonist. Cytosolic Ca^{2+} increase can related with cell apoptosis, and ER stress, and these processes will interactively further induce cytosolic Ca^{2+} increase via regulating Ca^{2+} gate by promoting the Ca^{2+} leaking from the plasma membrane or ER, and lower intracellular Ca^{2+} concentrations was associated with reduced apoptosis in inflammation (Germande et al., 2022; Liu Q. et al., 2022; Martinez-Carrasco et al., 2022). The results indicated that *PyTRPA1*-like might be involved in UPR and apoptosis by regulating cytoplasmic Ca^{2+} in scallops (Figure 11).

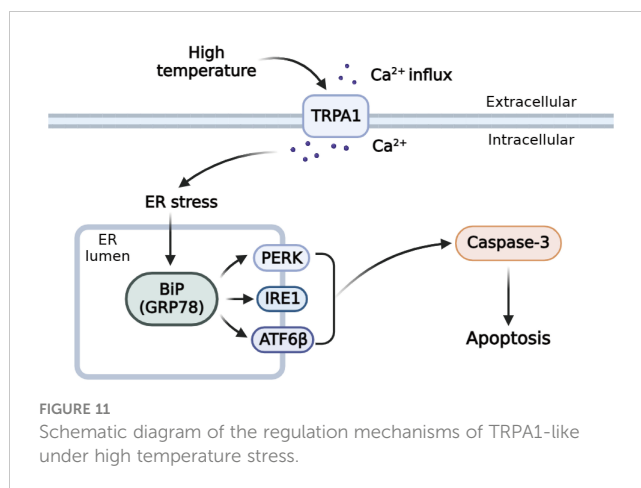


FIGURE 11
Schematic diagram of the regulation mechanisms of TRPA1-like under high temperature stress.

5 Conclusion

In conclusion, *PyTRPA1*-like with typical structural characteristics of vertebrate TRPA1 was identified in Yesso scallop. The mRNA transcripts of *PyTRPA1*-like were detected in haemocytes and all the examined tissues with the highest expression level in the mantle. After AITC and high temperature treatment, the transcripts of *PyTRPA1*-like, *PyGRP78*, *PyIRE1*, *PyATF6 β* , *PyPERK*, and *PyCaspase-3*, as well as Ca^{2+} content, and Caspase-3 activity and apoptosis rate in haemocytes increased significantly. And the decreased Ca^{2+} content, UPR related gene expression, and apoptosis rate were observed after *PyTRPA1*-like was inhibited by TRPA1 antagonist HC-030031. These results collectively indicated that *PyTRPA1*-like plays an important role in regulating Ca^{2+} influx, UPR and apoptosis, in the stress response of scallop *P. yessoensis*.

Data availability statement

The original contributions presented in the study are included in the article/Supplementary Materials. Further inquiries can be directed to the corresponding authors.

Ethics statement

The animal study was approved by the Ethics Review Committee of Dalian Ocean University. The study was conducted in accordance with the local legislation and institutional requirements.

Author contributions

XM: Methodology, Resources, Writing – review & editing, Data curation, Formal Analysis, Investigation, Project administration, Validation, Writing – original draft. WG: Data curation, Resources, Validation, Writing – review & editing. CY: Conceptualization, Funding acquisition, Methodology, Resources, Visualization,

Writing – review & editing. ZH: Data curation, Resources, Writing – review & editing. HF: Resources, Validation, Writing – review & editing. LW: Conceptualization, Funding acquisition, Resources, Supervision, Writing – review & editing. LS: Funding acquisition, Methodology, Writing – review & editing.

Funding

The author(s) declare financial support was received for the research, authorship, and/or publication of this article. This research was supported by a grant from National Natural Science Foundation of China (32373170), the fund for CARS-49 and for Outstanding Talents and Innovative Team of Agricultural Scientific Research in MARA, the Fund for General Scientific Research Projects in Higher Education Institutions of Educational Department of Liaoning Province (LJKMZ20221093), the innovation team of Aquaculture Environment Safety from Liaoning Province (LT20209), and Dalian High Level Talent Innovation Support Programs (2017RQ014 and 2022RG14).

Acknowledgments

We are grateful to all the laboratory members for their technical advice and helpful discussions.

Conflict of interest

The authors declare that the research was conducted in the absence of any commercial or financial relationships that could be construed as a potential conflict of interest.

The author(s) declared that they were an editorial board member of *Frontiers*, at the time of submission. This had no impact on the peer review process and the final decision.

References

- Bhardwaj, M., Leli, N. M., Koumenis, C., and Amaravadi, R. K. (2020). Regulation of autophagy by canonical and non-canonical ER stress responses. *Semin. Cancer Biol.* 66, 116–128. doi: 10.1016/j.semcancer.2019.11.007
- Buijs, T. J., and McNaughton, P. A. (2020). The role of cold-sensitive ion channels in peripheral thermosensation. *Front. Cell. Neurosci.* 14. doi: 10.3389/fncel.2020.00262
- Chiang, W. C., Hiramatsu, N., Messah, C., Kroeger, H., and Lin, J. H. (2012). Selective activation of ATF6 and PERK endoplasmic reticulum stress signaling pathways prevent mutant rhodopsin accumulation. *Invest. Ophthalmol. Visual Sci.* 53, 7159–7166. doi: 10.1167/iovs.12-10222
- Cordero-Morales, J. F., Gracheva, E. O., and Julius, D. (2011). Cytoplasmic ankyrin repeats of transient receptor potential A1 (TRPA1) dictate sensitivity to thermal and chemical stimuli. *Proc. Natl. Acad. Sci.* 108, E1184–E1191. doi: 10.1073/pnas.1114124108
- de Alba, G., Lopez-Olmeda, J. F., and Sanchez-Vazquez, F. J. (2021). Rearing temperature conditions (constant vs. thermocycle) affect daily rhythms of thermal tolerance and sensing in zebrafish. *J. Thermal. Biol.* 97, 102880. doi: 10.1016/j.jtherbio.2021.102880
- Ding, J., Yu, Y., Yang, M., Shi, D., Li, Z., Chi, X., et al. (2019). TRPA1 expression provides new insights into thermal perception by the sea urchin *Strongylocentrotus intermedius*. *J. Mar. Biol. Assoc. United Kingdom* 99, 1825–1829. doi: 10.1017/S0025315419000882
- Doerner, J. F., Gisselmann, G., Hatt, H., and Wetzel, C. H. (2007). Transient receptor potential channel A1 is directly gated by calcium ions. *J. Biol. Chem.* 282, 13180–13189. doi: 10.1074/jbc.M607849200
- Doihara, H., Nozawa, K., Kawabata-Shoda, E., Kojima, R., Yokoyama, T., and Ito, H. (2009). Molecular cloning and characterization of dog TRPA1 and AITC stimulate the gastrointestinal motility through TRPA1 in conscious dogs. *Eur. J. Pharmacol.* 617, 124–129. doi: 10.1016/j.ejphar.2009.06.038
- Eid, S. R., Crown, E. D., Moore, E. L., Liang, H. A., Choong, K.-C., Dima, S., et al. (2008). HC-030031, a TRPA1 selective antagonist, attenuates inflammatory-and neuropathy-induced mechanical hypersensitivity. *Mol. Pain* 4, 1744–8069. doi: 10.1186/1744-8069-4-48
- Eletto, D., Eletto, D., Dersh, D., Gidalevitz, T., and Argon, Y. (2014). Protein disulfide isomerase A6 controls the decay of IRE1 α signaling via disulfide-dependent association. *Mol. Cell.* 53, 562–576. doi: 10.1016/j.molcel.2014.01.004
- Ge, W., Huang, S., Liu, S., Sun, J., Liu, Z., Yang, W., et al. (2020). A novel Adiponectin receptor (AdipoR) involved in regulating cytokines production and apoptosis of haemocytes in oyster *Crassostrea gigas*. *Dev. Comp. Immunol.* 110, 103727. doi: 10.1016/j.dci.2020.103727
- Germande, O., Baudrimont, M., Beaufls, F., Freund-Michel, V., Ducret, T., Quignard, J.-F., et al. (2022). NiONPs-induced alteration in calcium signaling and mitochondrial function in pulmonary artery endothelial cells involves oxidative stress

Publisher's note

All claims expressed in this article are solely those of the authors and do not necessarily represent those of their affiliated organizations, or those of the publisher, the editors and the reviewers. Any product that may be evaluated in this article, or claim that may be made by its manufacturer, is not guaranteed or endorsed by the publisher.

Supplementary material

The Supplementary Material for this article can be found online at: <https://www.frontiersin.org/articles/10.3389/fmars.2024.1388382/full#supplementary-material>

SUPPLEMENTARY FIGURE S1

Multiple sequence alignment of PyTRPA1-like with TRPA1s from other species. The identical amino acid residues of TRPA1s are shaded in black, and similar amino acids are shaded in dark gray. The ANK of PyTRPA1 is marked with green backgrounds, and the transmembrane of PyTRPA1 domain is marked with purple backgrounds. The ANK of *H. sapiens* TRPA1 is marked with blue backgrounds, and the transmembrane domain of *H. sapiens* TRPA1 is marked with yellow backgrounds.

SUPPLEMENTARY FIGURE S2

Phylogenetic evolution of PyTRPA1-like with other TRP subfamily members. PyTRPA1-like is marked with a red circle. Sequence information of eleven TRPs are described in [Supplementary Table S1](#). Branches of different subfamily are highlighted with different color. TRPM subfamily, purple. TRPC subfamily, pink. TRPA subfamily, yellow. TRPV subfamily, blue. TRPP subfamily, green. TRPML subfamily, orange.

SUPPLEMENTARY FIGURE S3

Phylogenetic evolution of PyTRPA1-like with other TRP subfamily members. The PyTRPA1-like is marked with a red circle. Sequences information of all TRPAs are listed in [Supplementary Table S2](#).

SUPPLEMENTARY TABLE S1

Sequences used for the TRPs alignment and phylogenetic analysis.

SUPPLEMENTARY TABLE S2

Sequences used for the PyTRPA1-like alignment and phylogenetic analysis.

- and TRPV4 channels disruption. *Nanotoxicology* 16, 29–51. doi: 10.1080/17435390.2022.2030821
- Gupta, R., Saito, S., Mori, Y., Itoh, S. G., Okumura, H., and Tominaga, M. (2016). Structural basis of TRPA1 inhibition by HC-030031 utilizing species-specific differences. *Sci. Rep.* 6, 37460. doi: 10.1038/srep37460
- Himmel, N. J., and Cox, D. N. (2020). Transient receptor potential channels: current perspectives on evolution, structure, function and nomenclature. *Proc. R. Soc. B.* 287, 1273–1278. doi: 10.1098/rspb.2020.1309
- Ibrahim, I. M., Abdelmalek, D. H., and Elfiky, A. A. (2019). GRP78: A cell's response to stress. *Life Sci.* 226, 156–163. doi: 10.1016/j.lfs.2019.04.022
- Jaquemar, D., Schenker, T., and Trueb, B. (1999). An ankyrin-like protein with transmembrane domains is specifically lost after oncogenic transformation of human fibroblasts. *J. Biol. Chem.* 274, 7325–7333. doi: 10.1074/jbc.274.11.7325
- Jia, Z., Zhang, T., Jiang, S., Wang, M., Cheng, Q., Sun, M., et al. (2015). An integrin from oyster *Crassostrea gigas* mediates the phagocytosis toward *Vibrio splendidus* through LPS binding activity. *Dev. Comp. Immunol.* 53, 253–264. doi: 10.1016/j.dci.2015.07.014
- Karashima, Y., Talavera, K., Everaerts, W., Janssens, A., Kwan, K. Y., Vennekens, R., et al. (2009). TRPA1 acts as a cold sensor *in vitro* and *in vivo*. *Proc. Natl. Acad. Sci.* 106, 1273–1278. doi: 10.1073/pnas.0808487106
- Kashio, M., and Tominaga, M. (2022). TRP channels in thermosensation. *Curr. Opin. Neurobiol.* 75, 102591. doi: 10.1016/j.conb.2022.102591
- Kozma, M. T., Ngo-Vu, H., Wong, Y. Y., Shukla, N. S., Pawar, S. D., Senatore, A., et al. (2020). Comparison of transcriptomes from two chemosensory organs in four decapod crustaceans reveals hundreds of candidate chemoreceptor proteins. *PLoS One* 15, e0230266. doi: 10.1371/journal.pone.0230266
- Kozma, M. T., Schmidt, M., Ngo-Vu, H., Sparks, S. D., Senatore, A., and Derby, C. D. (2018). Chemoreceptor proteins in the Caribbean spiny lobster, *Panulirus argus*: expression of ionotropic receptors, gustatory receptors, and TRP channels in two chemosensory organs and brain. *PLoS One* 13, e0203935. doi: 10.1371/journal.pone.0203935
- Kurganov, E., Zhou, Y., Saito, S., and Tominaga, M. (2014). Heat and AITC activate green anole TRPA1 in a membrane-delimited manner. *Pflügers Archiv. European J. Physiol.* 466, 1873–1884. doi: 10.1007/s00424-013-1420-z
- Landini, L., Souza Monteiro de Araujo, D., Titiz, M., Geppetti, P., Nassini, R., and De Logu, F. (2022). TRPA1 role in inflammatory disorders: what is known so far? *Int. J. Mol. Sci.* 23, 4529. doi: 10.3390/ijms23094529
- Laursen, W. J., Anderson, E. O., Hoffstaetter, L. J., Bagriantsev, S. N., and Gracheva, E. O. (2015). Species-specific temperature sensitivity of TRPA1. *Temperature* 2, 214–226. doi: 10.1080/23328940.2014.1000702
- Lee, A. S. (2005). The ER chaperone and signaling regulator GRP78/BiP as a monitor of endoplasmic reticulum stress. *Methods* 35, 373–381. doi: 10.1016/j.jymeth.2004.10.010
- Li, R., Bai, S., Yang, D., and Dong, C. (2019). A crayfish Ras gene is involved in the defense against bacterial infection under high temperature. *Fish Shellfish Immunol.* 86, 608–617. doi: 10.1016/j.fsi.2018.11.062
- Li, R., Qi, J., Hu, L., Huang, J., Yang, J., Lin, R., et al. (2023). Molecular characterization of TRPA1 and its function in temperature preference in *Eriocheir sinensis*. *Comp. Biochem. Physiol. Part A: Mol. Integr. Physiol.* 278, 111357. doi: 10.1016/j.cbpa.2022.111357
- Li, Q., Xu, K., and Yu, R. (2007). Genetic variation in Chinese hatchery populations of the Japanese scallop (*Patinopecten yessoensis*) inferred from microsatellite data. *Aquaculture* 269, 211–219. doi: 10.1016/j.aquaculture.2007.04.017
- Lin, C., Liu, X., Sun, L., Liu, S., Sun, J., Zhang, L., et al. (2020). Effects of different flow velocities on behavior and TRPA1 expression in the sea cucumber *Apostichopus japonicus*. *J. Oceanol. Limnol.* 38, 1328–1340. doi: 10.1007/s00343-020-0061-2
- Liu, Q., Guo, S., Huang, Y., Wei, X., Liu, L., Huo, F., et al. (2022). Inhibition of TRPA1 ameliorates periodontitis by reducing periodontal ligament cell oxidative stress and apoptosis via PERK/eIF2 α /ATF-4/CHOP signal pathway. *Oxid. Med. Cell. Longev.* 2022, 4107915. doi: 10.1155/2022/4107915
- Liu, B., Song, X., Bai, S., and Dong, C. (2022). Crayfish (*Procambarus clarkii*) TRPA1 is required for the defense against *Aeromonas hydrophila* infection under high temperature conditions and contributes to heat sensing. *Comp. Biochem. Physiol. Part B: Biochem. Mol. Biol.* 257, 110654. doi: 10.1016/j.cbpb.2021.110654
- Liu, S., Wang, W., Ge, W., Lv, X., Han, Z., Li, Y., et al. (2020). An activating transcription factor 6 beta (ATF6 β) regulates apoptosis of hemocyte during immune response in *Crassostrea gigas*. *Fish Shellfish Immunol.* 99, 442–451. doi: 10.1016/j.fsi.2020.02.042
- Logashina, Y. A., Korolkova, Y. V., Kozlov, S., and Andreev, Y. A. (2019). TRPA1 channel as a regulator of neurogenic inflammation and pain: structure, function, role in pathophysiology, and therapeutic potential of ligands. *Biochem. (Moscow)* 84, 101–118. doi: 10.1134/S00066297919020020
- Mahajan, N., Khare, P., Kondepudi, K. K., and Bishnoi, M. (2021). TRPA1: Pharmacology, natural activators and role in obesity prevention. *Eur. J. Pharmacol.* 912, 174553. doi: 10.1016/j.ejphar.2021.174553
- Mahoney, J. L., Graugnard, E. M., Mire, P., and Watson, G. M. (2011). Evidence for involvement of TRPA1 in the detection of vibrations by hair bundle mechanoreceptors in sea anemones. *J. Comp. Physiol. A* 197, 729–742. doi: 10.1007/s00359-011-0636-7
- Martinez-Carrasco, R., Pablo, Argüeso, and Fini, M. E. (2022). Corrigendum to “Dyasore protects ocular surface mucosal epithelia subjected to oxidative stress by maintaining UPR and calcium homeostasis” [Free Radic. Biol. Med. 160 (2020) 57–66]. *Free Radical Biol. Med.* 179, 421–425. doi: 10.1016/j.freeradbiomed.2021.10.030
- Moparthi, L., Kichko, T. I., Eberhardt, M., Högestätt, E. D., Kjellbom, P., Johanson, U., et al. (2016). Human TRPA1 is a heat sensor displaying intrinsic U-shaped thermosensitivity. *Sci. Rep.* 6, 28763. doi: 10.1038/srep28763
- Naert, R., Talavera, A., Startek, J. B., and Talavera, K. (2020). TRPA1 gene variants hurting our feelings. *Pflügers Archiv. European J. Physiol.* 472, 953–960. doi: 10.1007/s00424-020-02397-y
- Nilius, B., Appendino, G., and Owsianik, G. (2012). The transient receptor potential channel TRPA1: from gene to pathophysiology. *Pflügers Archiv. European J. Physiol.* 464, 425–458. doi: 10.1007/s00424-012-1158-z
- Nilius, B., and Flockerzi, V. (2014). Mammalian transient receptor potential (TRP) cation channels (Berlin: Springer Science & Business Media). doi: 10.1007/978-3-642-54215-2
- Nilius, B., and Owsianik, G. (2011). The transient receptor potential family of ion channels. *Genome Biol.* 12, 1–11. doi: 10.1186/gb-2011-12-3-218
- Oda, M., Kubo, Y., and Saitoh, O. (2018). Sensitivity of Takifugu TRPA1 to thermal stimulations analyzed in oocytes expression system. *Neuroreport* 29, 280–285. doi: 10.1097/WNR.0000000000000939
- Oda, M., Kurogi, M., Kubo, Y., and Saitoh, O. (2016). Sensitivities of two zebrafish TRPA1 paralogs to chemical and thermal stimuli analyzed in heterologous expression systems. *Chem. Sens.* 41, 261–272. doi: 10.1093/chemse/bjv091
- Pandey, V. K., Mathur, A., and Kakkar, P. (2019). Emerging role of Unfolded Protein Response (UPR) mediated proteotoxic apoptosis in diabetes. *Life Sci.* 216, 246–258. doi: 10.1016/j.lfs.2018.11.041
- Paulsen, C. E., Armache, J. P., Gao, Y., Cheng, Y., and Julius, D. (2015). Structure of the TRPA1 ion channel suggests regulatory mechanisms. *Nature* 520, 511–517. doi: 10.1038/nature14367
- Peng, C., Yang, Z., Liu, Z., Wang, S., Yu, H., Cui, C., et al. (2021). A Systematical Survey on the TRP Channels Provides New Insight into Its Functional Diversity in Zhikong Scallop (*Chlamys farreri*). *Int. J. Mol. Sci.* 22, 11075. doi: 10.3390/ijms222011075
- Prober, D. A., Zimmerman, S., Myers, B. R., Mcdermott, B. M., Kim, S. H., Caron, S., et al. (2008). Zebrafish TRPA1 channels are required for chemosensation but not for thermosensation or mechanosensory hair cell function. *J. Neurosci.* 28, 10102–10110. doi: 10.1523/JNEUROSCI.2740-08.2008
- Qin, C., He, B., Dai, W., Lin, Z., Zhang, H., Wang, X., et al. (2014). The impact of a chlorotoxin-modified liposome system on receptor MMP-2 and the receptor-associated protein CIC-3. *Biomaterials* 35, 5908–5920. doi: 10.1016/j.biomaterials.2014.03.077
- Sághy, É., Sipos, É., Ács, P., Bölskei, K., Pohoczky, K., Kemeny, A., et al. (2016). TRPA1 deficiency is protective in cuprizone-induced demyelination—A new target against oligodendrocyte apoptosis. *Glia* 64, 2166–2180. doi: 10.1002/2016.23051
- Saito, S., Hamanaka, G., Kawai, N., Furukawa, R., Gojobori, J., Tominaga, M., et al. (2015). Functional diversity and evolutionary dynamics of thermoTRP channels. *Cell Calcium* 57, 214–221. doi: 10.1016/j.ceca.2014.12.001
- Saito, S., Hamanaka, G., Kawai, N., Furukawa, R., Gojobori, J., Tominaga, M., et al. (2017). Characterization of TRPA channels in the starfish *Patiria pectinifera*: involvement of thermally activated TRPA1 in thermotaxis in marine planktonic larvae. *Sci. Rep.* 7, 1–14. doi: 10.1038/s41598-017-02171-8
- Samad, A., Sura, L., Benedikt, J., Ettrich, R., Minofar, B., Teisinger, J., et al. (2011). The C-terminal basic residues contribute to the chemical- and voltage-dependent activation of TRPA1. *Biochem. J.* 433, 197–204. doi: 10.1042/BJ20101256
- Santamaria, P. G., Mazón, M. J., Eraso, P., and Portillo, F. (2019). UPR: an upstream signal to EMT induction in cancer. *J. Clin. Med.* 8, 624. doi: 10.3390/jcm8050624
- Schmidt, M., Dubin, A. E., Petrus, M. J., Earley, T. J., and Patapoutian, A. (2009). Nociceptive signals induce trafficking of TRPA1 to the plasma membrane. *Neuron* 64, 498–509. doi: 10.1016/j.neuron.2009.09.030
- Shamu, C. E., and Walter, P. (1996). Oligomerization and phosphorylation of the Ire1p kinase during intracellular signaling from the endoplasmic reticulum to the nucleus. *EMBO J.* 15, 3028–3039. doi: 10.1002/emboj.1996.15.issue-12
- Sinica, V., and Vlachová, V. (2021). Transient receptor potential ankyrin 1 channel: an evolutionarily tuned thermosensor. *Physiol. Res.* 70, 363. doi: 10.33549/physiolres.934697
- Stevens, J. S., Padilla, S., DeMarini, D. M., Hunter, D. L., Martin, W. K., Thompson, L. C., et al. (2018). Zebrafish locomotor responses reveal irritant effects of fine particulate matter extracts and a role for TRPA1. *Toxicol. Sci.* 161, 290–299. doi: 10.1093/toxsci/kfx217
- Story, G. M., Peier, A. M., Reeve, A. J., Eid, S. R., Mosbacher, J., Hricik, T. R., et al. (2003). ANKTM1, a TRP-like channel expressed in nociceptive neurons, is activated by cold temperatures. *Cell* 112, 819–829. doi: 10.1016/S0092-8674(03)00158-2
- Sura, L., Zima, V., Marsakova, L., Hynkova, A., Barvik, I., and Vlachova, V. (2012). C-terminal acidic cluster is involved in Ca²⁺-induced regulation of human transient receptor potential ankyrin 1 channel. *J. Biol. Chem.* 287, 18067–18077. doi: 10.1074/jbc.M112.341859
- Tabas, I., and Ron, D. (2011). Integrating the mechanisms of apoptosis induced by endoplasmic reticulum stress. *Nat. Cell Biol.* 13, 184–190. doi: 10.1038/ncb0311-184

- Talavera, K., Startek, J. B., Alvarez-Collazo, J., Boonen, B., Alpizar, Y. A., Sanchez, A., et al. (2020). Mammalian transient receptor potential TRPA1 channels: from structure to disease. *Physiol. Rev.* 100, 725–803. doi: 10.1152/physrev.00005.2019
- Tamura, K., Dudley, J., Nei, M., and Kumar, S. (2007). MEGA4: molecular evolutionary genetics analysis (MEGA) software version 4.0. *Mol. Biol. Evol.* 24, 1596–1599. doi: 10.1093/molbev/msm092
- Wagner, E. M. (2013). Monitoring gene expression: quantitative real-time rt-PCR. *Lipoproteins Cardiovasc. Dis.: Methods Protoc.*, 19–45. doi: 10.1007/978-1-60327-369-5_2
- Wang, Y. Y., Chang, R. B., Waters, H. N., McKemy, D. D., and Liman, E. R. (2008). The nociceptor ion channel TRPA1 is potentiated and inactivated by permeating calcium ions. *J. Biol. Chem.* 283, 32691–32703. doi: 10.1074/jbc.M803568200
- Wang, W., Zhang, T., Wang, L., Xu, J., Li, M., Zhang, A., et al. (2016). A new non-phagocytic TLR6 with broad recognition ligands from Pacific oyster *Crassostrea gigas*. *Dev. Comp. Immunol.* 65, 182–190. doi: 10.1016/j.dci.2016.07.010
- Wu, Y., Shu, J., He, C., Li, M., Wang, Y., Ou, W., et al. (2016). ROCK inhibitor Y27632 promotes proliferation and diminishes apoptosis of marmoset induced pluripotent stem cells by suppressing expression and activity of caspase 3. *Theriogenology* 85, 302–314. doi: 10.1016/j.theriogenology.2015.09.020
- Wu, Y., Yang, C., Liu, D., Lu, M., Lu, G., Sun, J., et al. (2018). Inositol-requiring enzyme 1 involved in regulating hemocyte apoptosis upon heat stress in *Patinopecten yessoensis*. *Fish Shellfish Immunol.* 78, 248–258. doi: 10.1016/j.fsi.2018.04.048
- Yang, C., Gao, Q., Liu, C., Wang, L., Zhou, Z., Gong, C., et al. (2017). The transcriptional response of the Pacific oyster *Crassostrea gigas* against acute heat stress. *Fish Shellfish Immunol.* 68, 132–143. doi: 10.1016/j.fsi.2017.07.016
- Yang, C., Guo, X., Shan, Y., He, Z., Jiang, D., Wang, X., et al. (2021). The expression profile of calnexin in *Patinopecten yessoensis* after acute high temperature stress. *Fish Shellfish Immunol. Rep.* 2, 100016. doi: 10.1016/j.fsirep.2021.100016
- Yin, S., Zhang, L., Ding, L., Huang, Z., Xu, B., Li, X., et al. (2018). Transient receptor potential ankyrin 1 (trpa1) mediates il-1 β -induced apoptosis in rat chondrocytes via calcium overload and mitochondrial dysfunction. *J. Inflamm.* 15, 1–9. doi: 10.1186/s12950-018-0204-9
- Yu, B., Qiao, Z., Cui, J., Lian, M., Han, Y., Zhang, X., et al. (2021). A host-coupling bio-nanogenerator for electrically stimulated osteogenesis. *Biomaterials* 276, 120997. doi: 10.1016/j.biomaterials.2021.120997
- Zhang, S., Hu, S., Dong, W., Huang, S., Jiao, Z., Hu, Z., et al. (2023). Prenatal dexamethasone exposure induces anxiety-and depressive-like behavior of male offspring rats through intrauterine programming of the activation of NRG1-ErbB4 signaling in hippocampal PV interneurons. *Cell Biol. Toxicol.* 39, 657–678. doi: 10.1007/s10565-021-09621-0
- Zhao, L., Wang, S., Liu, H., Du, X., Bu, R., Li, B., et al. (2021). The pharmacological effect and mechanism of lanthanum hydroxide on vascular calcification caused by chronic renal failure hyperphosphatemia. *Front. Cell Dev. Biol.* 9. doi: 10.3389/fcell.2021.639127